Impact of stratospheric ozone on Southern Hemisphere circulation change: A multimodel assessment

S.-W. Son,[1] E. P. Gerber,[2] J. Perlwitz,[3,4] L. M. Polvani,[5,6] N. P. Gillett,[7] K.-H. Seo,[8] V. Eyring,[9] T. G. Shepherd,[10] D. Waugh,[11] H. Akiyoshi,[12] J. Austin,[13] A. Baumgaertner,[14] S. Bekki,[15] P. Braesicke,[16] C. Brühl,[14] N. Butchart,[17] M. P. Chipperfield,[18] D. Cugnet,[15] M. Dameris,[9] S. Dhomse,[18] S. Frith,[19] H. Garny,[9] R. Garcia,[20] S. C. Hardiman,[17] P. Jöckel,[9,14] J. F. Lamarque,[20] E. Mancini,[21] M. Marchand,[15] M. Michou,[22] T. Nakamura,[12] O. Morgenstern,[16,23] G. Pitari,[21] D. A. Plummer,[24] J. Pyle,[16] E. Rozanov,[25,26] J. F. Scinocca,[7] K. Shibata,[27] D. Smale,[23] H. Teyssèdre,[22] W. Tian,[18] and Y. Yamashita[12]

Received 27 March 2010; revised 16 June 2010; accepted 7 July 2010; published 13 October 2010.

[1] The impact of stratospheric ozone on the tropospheric general circulation of the Southern Hemisphere (SH) is examined with a set of chemistry-climate models participating in the Stratospheric Processes and their Role in Climate (SPARC)/Chemistry-Climate Model Validation project phase 2 (CCMVal-2). Model integrations of both the past and future climates reveal the crucial role of stratospheric ozone in driving SH circulation change: stronger ozone depletion in late spring generally leads to greater poleward displacement and intensification of the tropospheric midlatitude jet, and greater expansion of the SH Hadley cell in the summer. These circulation changes are systematic as poleward displacement of the jet is typically accompanied by intensification of the jet and expansion of the Hadley cell. Overall results are compared with coupled models participating in the Intergovernmental Panel on Climate Change Fourth Assessment Report (IPCC AR4), and possible mechanisms are discussed. While the tropospheric circulation response appears quasi-linearly related to stratospheric ozone changes, the quantitative response to a given forcing varies considerably from one model to another. This scatter partly results from differences in model climatology. It is shown that poleward intensification of the westerly jet is generally stronger in models whose climatological jet is biased toward lower latitudes. This result is discussed in the context of quasi-geostrophic zonal mean dynamics.

Citation: Son, S.-W., et al. (2010), Impact of stratospheric ozone on Southern Hemisphere circulation change: A multimodel assessment, *J. Geophys. Res.*, *115*, D00M07, doi:10.1029/2010JD014271.

[1]Department of Atmospheric and Oceanic Sciences, McGill University, Montreal, Quebec, Canada.
[2]Center for Atmosphere Ocean Science, Courant Institute of Mathematical Sciences, New York University, New York, New York, USA.
[3]Cooperative Institute for Research in Environmental Sciences, University of Colorado at Boulder, Boulder, Colorado, USA.
[4]Physical Sciences Division, Earth System Research Laboratory, NOAA, Boulder, Colorado, USA.
[5]Department of Applied Physics and Applied Mathematics, Columbia University, New York, New York, USA.
[6]Department of Earth and Environmental Sciences, Columbia University, New York, New York, USA.
[7]Canadian Centre for Climate Modelling and Analysis, Environment Canada, University of Victoria, Victoria, British Columbia, Canada.
[8]Department of Atmospheric Sciences, Pusan National University, Pusan, South Korea.
[9]Deutsches Zentrum für Luft- und Raumfahrt, Institut für Physik der Atmosphäre, Oberpfaffenhofen, Germany.
[10]Department of Physics, University of Toronto, Toronto, Ontario, Canada.
[11]Department of Earth and Planetary Sciences, Johns Hopkins University, Baltimore, Maryland, USA.
[12]National Institute for Environmental Studies, Tsukuba, Japan.
[13]Geophysical Fluid Dynamics Laboratory, NOAA, Princeton, New Jersey, USA.
[14]Max Planck Institut für Chemie, Mainz, Germany.
[15]LATMOS, Institut Pierre-Simone Laplace, UVSQ, UPMC, CNRS/INSU, Paris, France.
[16]NCAS-Climate-Chemistry, Department of Chemistry, Cambridge University, Cambridge, UK.
[17]Met Office Hadley Centre, Exeter, UK.
[18]School of Earth and Environment, University of Leeds, Leeds, UK.
[19]NASA Goddard Space Flight Center, Greenbelt, Maryland, USA.
[20]Atmospheric Chemistry Division, National Center for Atmospheric Research, Boulder, Colorado, USA.
[21]Dipartimento di Fisica, Universita degli Studi de L'Aquila, L'Aquila, Italy.
[22]GAME/CNRM, Météo-France, Centre National de Recherches Météorologiques, Toulouse, France.
[23]National Institute of Water and Atmospheric Research, Lauder, New Zealand.
[24]Canadian Centre for Climate Modelling and Analysis, Environment Canada, Toronto, Ontario, Canada.
[25]Physikalisch-Meteorologisches Observatorium Davos/World Radiation Center, Davos, Switzerland.
[26]Institute for Atmospheric and Climate Science, ETH, Zurich, Switzerland.
[27]Meteorological Research Institute, Tsukuba, Japan.

Copyright 2010 by the American Geophysical Union.
0148-0227/10/2010JD014271

1. Introduction

[2] The atmospheric general circulation has been significantly altered in the recent past by anthropogenic climate forcing. Examples include intensification of the westerly jet on the poleward side of the climatological jet, which is often described as a positive trend in the annular modes [*Thompson et al.*, 2000; *Chen and Held*, 2007], and the poleward expansion (or widening) of the Hadley cell [*Fu et al.*, 2006; *Hu and Fu*, 2007; *Seidel et al.*, 2008; *Johanson and Fu*, 2009]. Although these changes are relatively weak, they have been extensively examined since they are directly related to changes in global hydrology, e.g., shifts in the extratropical storm tracks and subtropical arid regions [*Yin*, 2005; *Bengtsson et al.*, 2006; *Lu et al.*, 2007; *Seidel et al.*, 2008].

[3] Anthropogenic climate change has been exceptionally strong in the SH summer. While the index of the southern annular mode (SAM), for instance, has increased in most seasons in the recent past, the trend is strongest in the summer [*Thompson and Solomon*, 2002; *Marshall*, 2003; *Fogt et al.*, 2009]. This strong circulation change in austral summer has been attributed to increase in greenhouse gases (GHGs) and decrease in stratospheric ozone (O_3, hereafter O_3 denotes stratospheric ozone only) concentrations [*Thompson and Solomon*, 2002; *Gillett and Thompson*, 2003; *Shindell and Schmidt*, 2004; *Arblaster and Meehl*, 2006; *Miller et al.*, 2006; *Cai and Cowan*, 2007; *Perlwitz et al.*, 2008; *Son et al.*, 2008, 2009b]. It is known that both GHGs increase [e.g., *Fyfe et al.*, 2007; *Kushner et al.*, 2001] and O_3 loss [e.g., *Gillett and Thompson*, 2003; *Shindell and Schmidt*, 2004] drive the SH climate in the same direction, toward a positive trend of the SAM index. While the GHG-induced climate changes occur year round, O_3-induced changes occur primarily in the SH summer. Consequently, stronger trends are observed in the SH summer than in other seasons, or in the Northern Hemisphere (NH). It is expected, however, that the SH summer circulation changes will be substantially weaker, or even reversed, in the future because of the anticipated recovery of stratospheric O_3 resulting from the implementation of the Montreal Protocol [*Shindell and Schmidt*, 2004; *Perlwitz et al.*, 2008; *Son et al.*, 2008, 2009b].

[4] While there is no doubt that O_3 influences the climate of the SH, there are several outstanding questions about the relationship between stratospheric O_3 and the tropospheric circulation. In this study we use a comprehensive set of chemistry-climate model simulations of O_3 loss and recovery to address three principal concerns. First, we examine the impact of stratospheric O_3 changes on the tropospheric circulation of the *entire* Southern Hemisphere, from tropics to pole. Previous studies have primarily focused on the barotropic response to O_3 quantified by the SAM, and associated changes in surface temperature and wind. Less attention has been paid to broader changes in the atmospheric general circulation, including the subtropical circulation. *Son et al.* [2009a] suggested that the SH summer Hadley cell might be influenced by stratospheric O_3 change, but this link has not been investigated as carefully as its relationship to global warming [e.g., *Frierson et al.*, 2007; *Lu et al.*, 2008].

[5] Second, we establish a more *quantitative* relationship between stratospheric O_3 and tropospheric circulation changes. Most previous studies are based on sensitivity tests with a single climate model [e.g., *Gillett and Thompson*, 2003; *Shindell and Schmidt*, 2004; *Arblaster and Meehl*, 2006; *Perlwitz et al.*, 2008]. Although multimodel assessments have been conducted with coupled models participating in the Intergovernmental Panel on Climate Change (IPCC) Fourth Assessment Report (AR4), only qualitative insights have been obtained because the ozone fields were not archived for the IPCC AR4 models (hereafter AR4 models) and each modeling group had used different ozone forcing [*Cordero and Forster*, 2006; *Miller et al.*, 2006; *Cai and Cowan*, 2007; *Son et al.*, 2008]. *Son et al.* [2008] attempted to establish a quantitative relationship between stratospheric O_3 and tropospheric circulation changes in an earlier generation of chemistry-climate models, but their analysis was restricted to zonal wind changes in future climates. In this study, we analyze 17 chemistry-climate models participating in the Stratospheric Processes and their Role in Climate project (SPARC) Chemistry-Climate Model Validation phase 2 (CCMVal-2) report to quantitatively relate changes in stratospheric O_3 to those in the Hadley cell and westerly jet in simulations of both ozone loss and recovery. The results are compared with the AR4 models and previous investigations.

[6] The third and final goal of this study is to investigate the possible mechanisms by which stratospheric ozone, whose radiative forcing signature is relatively small at the surface, influences the tropospheric circulation. By testing possible mechanisms proposed in the literature using the SPARC CCMVal-2 model (hereafter CCMVal-2 model) output, we hope to gain better insights on the ozone-induced circulation changes in the SH.

[7] This paper is organized as follows. In section 2, we briefly describe the data and our methodology. In section 3, the CCMVal-2 models are evaluated against reanalysis data. This is followed by trend analyses of zonal winds, temperature, and other variables to establish the circulation response to southern polar cap O_3 change. In section 4, possible mechanisms of O_3-induced circulation changes are discussed. Lastly, a summary and additional discussion are given in section 5.

2. Data and Methodology

[8] The primary data used in this study are the CCMVal-2 model output. Since details on the CCMVal-2 models and their simulations are described by *Eyring et al.* [2008] and *Morgenstern et al.* [2010], only key aspects are introduced below. The CCMVal-2 models are state-of-the-art chemistry-climate models, designed to resolve both tropospheric and stratospheric processes. The model tops are typically placed at or above the stratopause, and stratospheric chemistry is fully interactive with radiation and dynamics. Tropospheric chemistry, however, is not simulated interactively in most models. All other physical processes are standard and comparable to those used in coupled models. An exception is the surface boundary condition: most CCMVal-2 models prescribe sea surface temperature and sea ice concentration. They are derived from the observations for the past climate integrations or the AR4 A1B GHGs scenario runs for the future climate integrations.

[9] A total of 17 models with all available ensemble members are analyzed in this study (Table 1). A coarse-

Table 1. CCMVal-2 Models Used in This Study[a]

Model Name	REF-B1 (1960–1999)	REF-B2 (2000–2079)	References
AMTRAC3	1		*Austin and Wilson* [2010]
CAM3.5	1	1	*Lamarque et al.* [2008]
CCSRNIES	1	1	*Akiyoshi et al.* [2009]
CMAM	3	3	*Scinocca et al.* [2008], *de Grandpré et al.* [2000]
CNRM-ACM	2	1	*Déqué* [2007], *Teyssédre et al.* [2007]
E39CA	1		*Stenke et al.* [2009], *Garny et al.* [2009]
EMAC	1		*Jöckel et al.* [2006]
GEOSCCM	1	1	*Pawson et al.* [2008]
LMDZrepro	3		*Jourdain et al.* [2008]
MRI	4	2	*Shibata and Deushi* [2008a, 2008b]
Niwa-SOCOL	1		*Schraner et al.* [2008], *Egorova et al.* [2005]
SOCOL	3	3	*Schraner et al.* [2008]
UMETRAC	1		*Austin and Butchart* [2003]
UMSLIMCAT	1	1	*Tian and Chipperfield* [2005], *Tian et al.* [2006]
UMUKCA-METO	1	1	*Morgenstern et al.* [2008, 2009]
UMUKCA-UCAM	1		*Morgenstern et al.* [2008, 2009]
WACCM	4	3	*Garcia et al.* [2007]

[a]Number of ensemble members is denoted in the second and third columns. See *Morgenstern et al.* [2010] for the details.

resolution model, with rhomboidal-6 truncation, is excluded from this study as it is not well suited for examining tropospheric circulation changes. Two reference integrations are examined. They are a base integration for the period of 1960–2006 (REF-B1) and a scenario integration for the period of 1960–2100 (REF-B2). The REF-B1 integrations are forced with observed GHGs, ozone depleting substances (ODSs), sea surface temperatures (SSTs), sea ice concentrations (SICs), solar variability, and aerosols including volcanic aerosols. The REF-B2 integrations are based on both observations and scenario forcings. The scenario forcing are applied after 2000; they are the A1B GHGs scenario, A1 ODSs scenario, modeled SSTs/SICs, and constant solar flux and background surface area density aerosol. See *Morgenstern et al.* [2010] for further details.

[10] Following the analysis of *Son et al.* [2009a], AR4 models from the Coupled Model Intercomparison Project 3 (CMIP3) [*Randall et al.*, 2007] are also examined and compared with the CCMVal-2 models. The AR4 models used in this study are identical to those from *Son et al.* [2009a] and listed in Table 2. A total of 20 models from both the 20C3M and A1B GHGs scenario integrations are analyzed, and all available ensemble members are used, as with the CCMVal-2 models. Note that, unlike the CCMVal-2 models, the AR4 models prescribe stratospheric O_3. The O_3 forcing, however, was applied differently in each model. Roughly half of the models (12 from the 20C3M and 10 from the A1B GHGs scenario integrations) prescribed stratospheric O_3 depletion in the past and recovery in the future, whereas the others used climatological O_3. Because of this, all analyses are performed separately for models with and without time-varying O_3 concentration, as in work by *Son et al.* [2009a]. Although the AR4 models differ from the CCMVal-2 models in many aspects (e.g., coarse versus fine vertical resolution in the stratosphere, prescribed versus interactive stratospheric O_3, coupled versus prescribed surface boundary conditions, etc.), we show below that overall results of the AR4 models are qualitatively similar to those of the CCMVal-2 models, provided that the former prescribe time varying O_3 forcing.

[11] Both model data sets are compared against reanalyses by the European Centre for Medium-Range Weather Forecasts (ERA40) [*Uppala et al.*, 2005] and the National Centers for Environmental Prediction–National Center for Atmospheric Research (NCEP-NCAR) [*Kalnay et al.*, 1996]. Due to limited observations in the SH before the satellite era, only reanalyses between 1979 and 1999 are used.

[12] Most results presented here are based on linear trends. Linear trends are first computed from monthly or seasonally averaged fields for each individual model realization with a least squares fit. The trend of a given model is calculated by averaging the trends of all available ensemble members. The analysis periods are 1960–1999 in the CCMVal-2 REF-B1 and AR4 20C3M integrations, and

Table 2. AR4 Models Used in This Study[a]

Model Name	20C3M (1960–1999)	A1B (2000–2079)
CSIRO Mk3.0	2 (Y)	1 (Y)
GFDL CM2.0	3 (Y)	1 (Y)
GFDL CM2.1	3 (Y)	1 (Y)
INGV SXG[b]	1 (Y)	1 (Y)
MIROC3.2(medres)[b]	3 (Y)	3 (Y)
MPI ECHAM5/MPI-OM[b]	4 (Y)	4 (Y)
NCAR CCSM3.0[b]	8 (Y)	7 (Y)
NCAR PCM1[b]	4 (Y)	4 (Y)
UKMO HadCM3[b]	2 (Y)	1 (Y)
UKMO HadGEM1[b]	2 (Y)	1 (Y)
GISS EH[b]	5 (Y)	3 (N)
GISS ER[b]	9 (Y)	5 (N)
BCCR BCM2.0	1 (N)	1 (N)
CCCma CGCM3.1(T63)	1 (N)	1 (N)
CNRM CM3[c]	1 (N)	1 (N)
GISS AOM	2 (N)	2 (N)
IAP FGOALS-g1.0	3 (N)	3 (N)
INM CM3.0	1 (N)	1 (N)
IPSL CM4	2 (N)	1 (N)
MRI CGCM2.3.2	5 (N)	5 (N)

[a]Models are identical to those used by *Son et al.* [2009a] and described by *Randall et al.* [2007]. The parenthesized Y or N in the second and third columns denotes the presence or absence of time-varying stratospheric ozone in each model.

[b]Models have prescribed ozone depletion and have seven or more vertical levels between 300 hPa and 10 hPa (see *Karpechko et al.* [2008]).

[c]Model documentation claims the inclusion of time-varying stratospheric ozone, but the Antarctic polar cap temperature does not show the ozone impact in either the 20C3M or A1B scenario integrations (see Figure 3c of *Son et al.* [2008]).

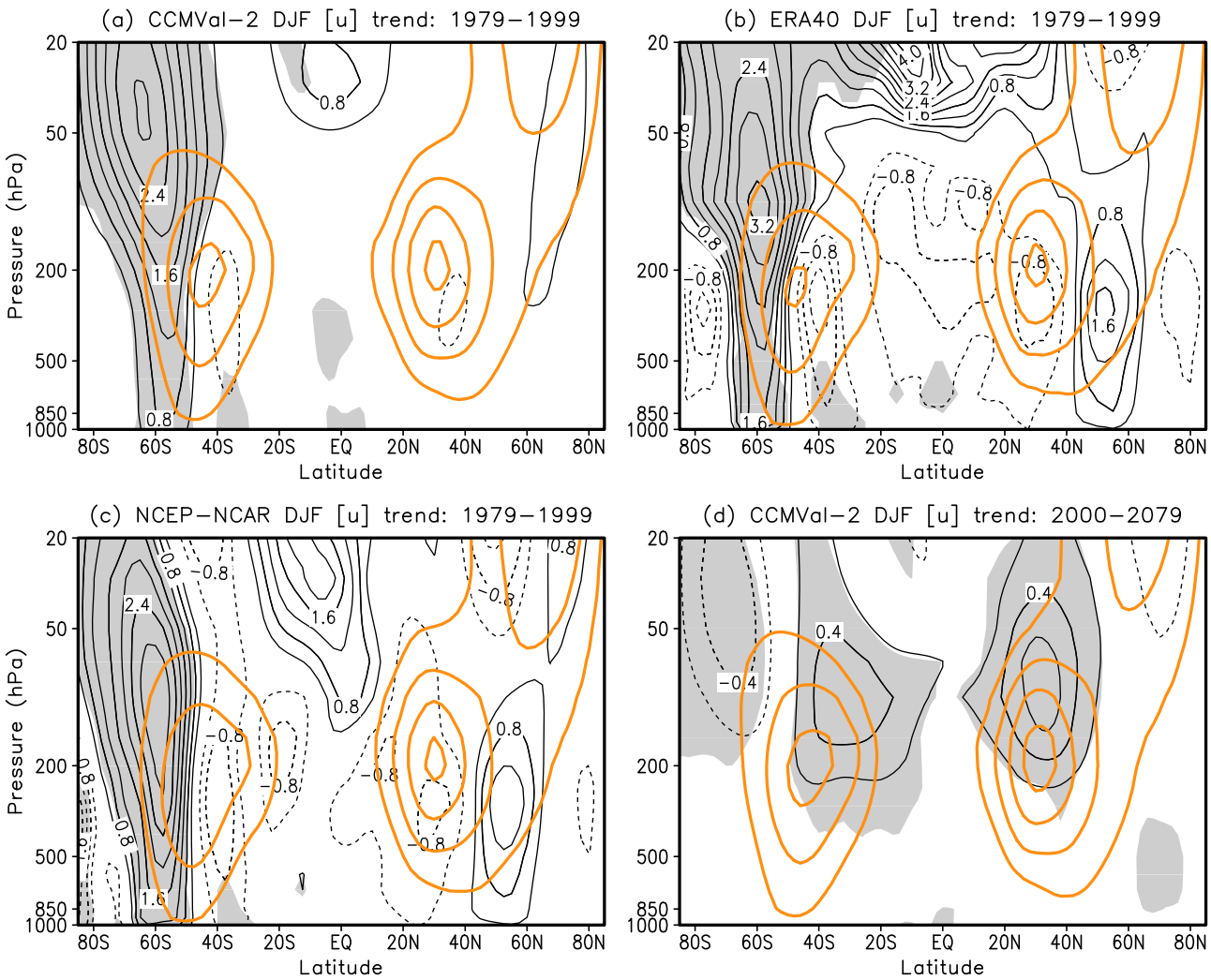

Figure 1. The long-term mean (thick orange) and linear trend (thin black contour) of DJF [*u*] over 1979–1999: (a) CCMVal-2 REF-B1 multimodel mean, (b) ERA40, and (c) NCEP-NCAR reanalysis data. (d) Future trends over 2000–2079 as simulated by the CCMVal-2 REF-B2 models. Contour intervals of climatological wind and trend are 10 m s^{-1} starting from 10 m s^{-1} and 0.4 m s^{-1}/decade, respectively. In Figures 1a and 1d, multimodel mean values exceeding 1 standard deviation are shaded. In Figures 1b and 1c, trends which are statistically significant at the 95% confidence level are shaded. Zero contours are omitted in all plots.

2000–2079 in the CCMVal-2 REF-B2 and AR4 A1B scenario integrations. An exception is section 3.1, where trends are calculated for the period 1979–1999 to be compared with reanalysis data, and for the period 2001–2050 to be compared with the previous CCMVal activity (CCMVal-1). Past climate changes are analyzed for a relatively long period of 40 years, mainly because O_3 depletion began before 1979; observations have shown that O_3 concentration started to decrease in the late 1960s, although early trends are quite weak [e.g., *Solomon*, 1999, Figure 1]. The longer period also allows us to obtain better statistics and compare our results with previous studies. The analysis length for future climate change is twice as long as that for past climate change because O_3 recovery is predicted to be slower than its depletion in the past. The CCMVal-2 models predict that total column O_3 over the Antarctic will likely reach its 1980 value around 2060 [*Austin et al.*, 2010]. Although the analysis period is somewhat subjective, results are only weakly sensitive to the choice of time period. It is found that trends over 2000–2049 are quantitatively similar to those over 2000–2079, although the intermodel standard deviation is somewhat larger.

[13] Stratospheric O_3 has strong seasonality and its long-term trend is largest in the late spring. Its impact on the tropospheric circulation, however, is delayed by a few months and reaches a maximum in the summer, December–February (DJF) [*Gillett and Thompson*, 2003; *Shindell and Schmidt*, 2004; *Perlwitz et al.*, 2008; *Son et al.*, 2008]. Hence, most analyses in this study are carried out for the SH summer.

3. Results

[14] We first evaluate the CCMVal-2 models by comparing the spatial and temporal structure of the zonal mean

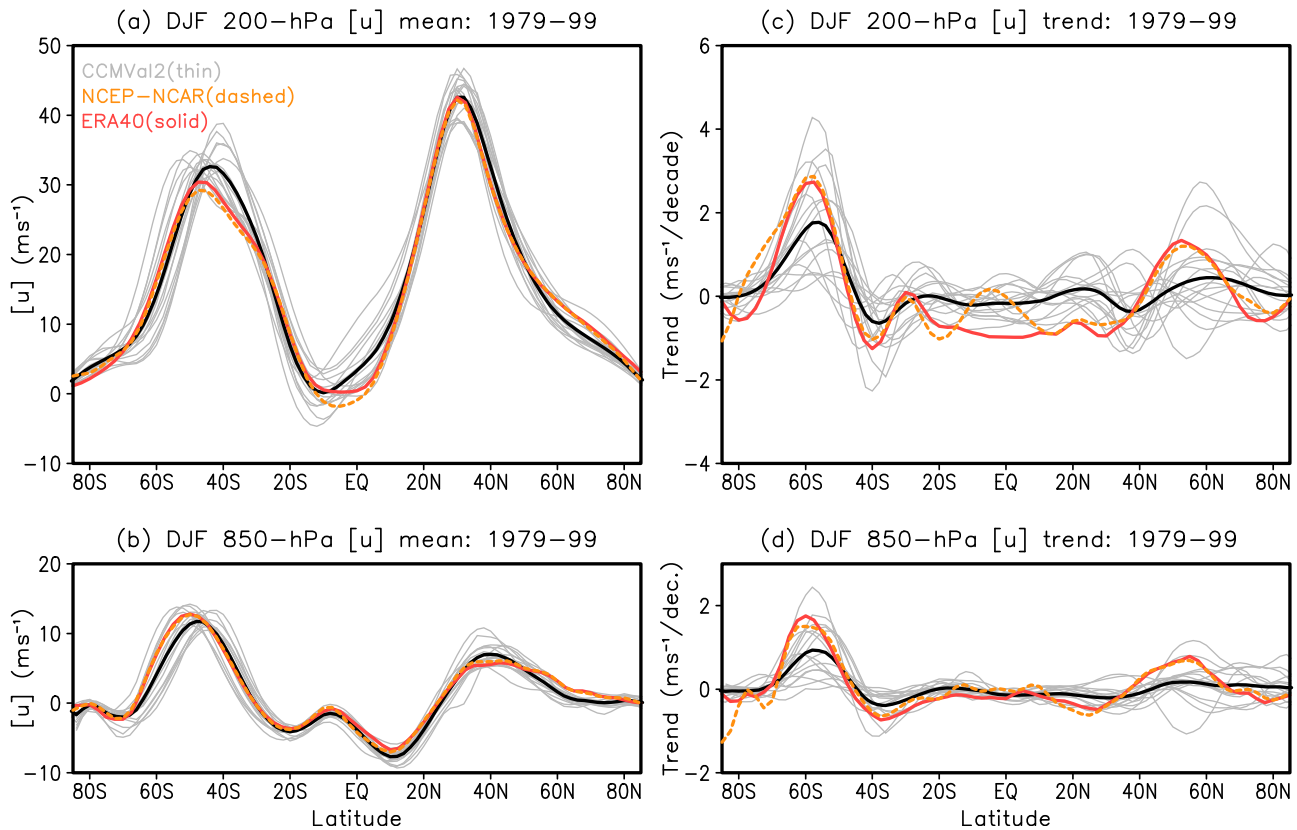

Figure 2. The long-term (left) mean and (right) trends of DJF [u] at (a, c) 200 hPa and (b, d) 850 hPa. The thin grey and thick black lines denote individual CCMVal-2 REF-B1 model integrations and multi-model mean, respectively.

zonal wind, [*u*], trends with reanalysis data. Figure 1a shows multimodel mean climatology (thick contour lines) and linear trend (thin contour lines) of DJF [*u*] for time period of 1979–1999. Multimodel mean trends which exceed 1 standard deviation of individual models' trends are shaded. Identical calculations were performed with the ERA40 and NCEP-NCAR reanalyses, and results are shown in Figures 1b and 1c where shading denotes trends which are statistically significant at the 95% confidence level in a Student's *t* test. The CCMVal-2 models successfully reproduce the spatial structure of the climatological jet and its recent trend. The poleward displacement of the SH jet, whose spatial structure is qualitatively similar to the zonal wind anomalies associated with the positive phase of the SAM (not shown), is particularly well reproduced.

[15] Each model is further evaluated by examining the DJF [*u*] climatology and trend at 200 and 850 hPa (Figure 2). Although the multimodel mean climatology looks reasonable, we note that over two third of models fail to reproduce the location of the SH jet: several models show the jet up to 10° north or south of the jet in the reanalysis data (Figures 2a and 2c). In addition, most models overestimate the intensity of the jet (Figures 2a and 2c). Long-term trends of DJF [u] also show notable differences among the models (Figures 2b and 2d). Model trends are generally weaker than trends derived from the reanalysis data, although the latter may overestimate trends in the SH [e.g., *Marshall*, 2003]. We note here that the comparison to reanalysis data is carried out to find qualitative similarity. The quantitative comparisons between the models and reanalyses in the SH need great caution, as the sparsity of observations draws into question the quality of the latter. In fact, although DJF [u] trends are comparable between the ERA40 and NCEP-NCAR reanalysis data (Figure 1), trends for other variables such as extratropical tropopause pressure and the latitude of the poleward boundary of the SH Hadley cell are substantially different. For instance, $\langle p_{trp} \rangle$ trends over 1979–1999 are −11.30 and −4.99 hPa/decade for the ERA40 and NCEP-NCAR reanalysis data, respectively [see also *Son et al.*, 2009a]. The $[H]_{lat}$ trends are 0.84 and −0.83 degrees/decades, respectively; they have opposite sign although the former is not statistically significant. These suggest that the reanalysis data are not well suited for trend analysis of the SH climate.

[16] It is noteworthy that in the NH the CCMVal-2 models faithfully reproduce the jet. The location and intensity of the climatological jet are remarkably similar to those in the reanalysis data (Figures 2a and 2c). However, long-term trends are somewhat underestimated, as in the SH (Figures 2b and 2d).

3.1. Vertical Structure of the SH Polar Climate Change

[17] Figure 3a shows the multimodel mean trend of polar cap O_3 as simulated by the CCMVal-2 REF-B1 integrations. The CCMVal-2 models successfully reproduce stratospheric O_3 depletion in the last 4 decades, which is qualitatively similar to observations [e.g., *Randel and Wu*, 1999]. In fact, it was shown that long-term trends of total column ozone in most CCMVal-2 models are to a large

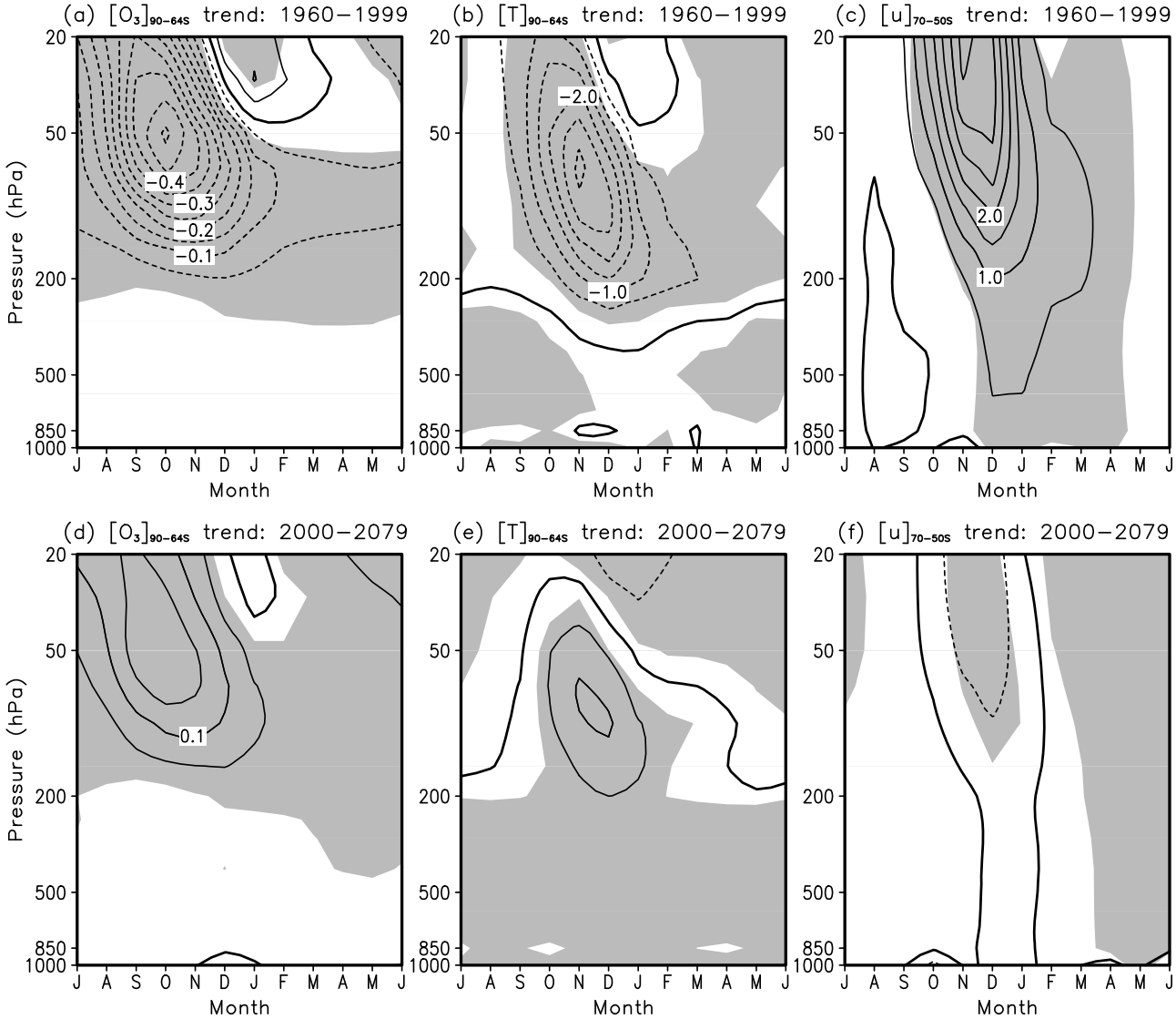

Figure 3. Linear trends of (a, d) the monthly mean [O_3], (b, e) [T] integrated south of 64°S, and (c, f) [u] integrated from 70° to 50°S. The multimodel mean trends are computed for the time period of 1960–1999 in the CCMVal-2 REF-B1 runs (Figures 3a–3c) and for the time period of 2000–2079 in the CCMVal-2 REF-B2 runs (Figures 3d–3f). Starting month in the x axis is July, and contour intervals are 0.05 ppmv/decade (Figures 3a and 3d), 0.5 K/decade (Figures 3b and 3e), and 0.5 m s^{-1}/decade (Figures 3c and 3f). Zero lines are denoted with thick black lines, and multimodel mean values exceeding 1 standard deviation are shaded.

degree comparable to those in the observations [*SPARC CCMVal*, 2010, chapter 10].

[18] Ozone depletion leads to radiative cooling in the lower stratosphere (Figure 3b) after a delay of 1 month; that is, the maximum O_3 depletion is in October whereas the maximum cooling is in November. This delay is consistent with observations [*Randel and Wu*, 1999; *Thompson and Solomon*, 2002] and likely caused by the relatively long radiative time scale in the lower stratosphere, which is about a month [e.g., *Thompson and Solomon*, 2002]. The cooling over the southern polar cap then accelerates the extratropical [u] (Figure 3c) by enhancing the zonal mean temperature [T] gradient. This acceleration, however, is not confined to the stratosphere. It penetrates all the way down to the surface after a lag of another 1 to 2 months. The result is a significant intensification of [u] in the lower troposphere during DJF (Figure 3c), as demonstrated in previous studies [e.g., *Perlwitz et al.*, 2008]. Note that [u] changes in other seasons are almost negligible. This suggests that tropospheric [u] in the SH extratropics has been driven more by stratospheric O_3 than tropospheric GHGs changes in the period of analysis [see also *Polvani et al.*, 2010].

[19] Figures 3d–3f show that future trends in the stratosphere have essentially the same structure as that in the past, but with the opposite sign and a much weaker magnitude [see also *Perlwitz et al.*, 2008]. In contrast to the past climate integrations, however, stratospheric [u] changes in the future climate integrations are not well linked to tropospheric [u] changes (compare Figures 3c and 3f; see also Figures 1a and 1d). A weak hint of deceleration is found in

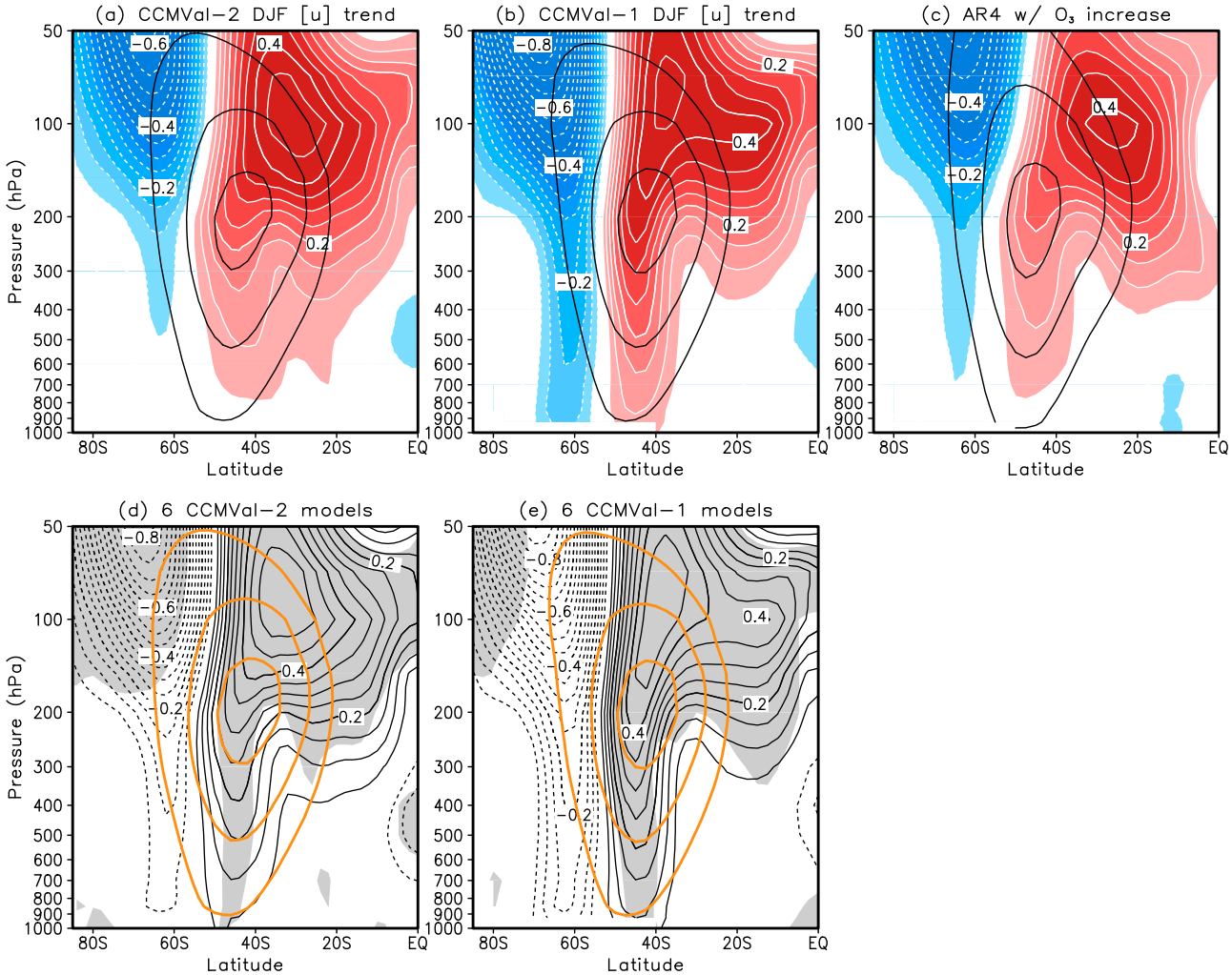

Figure 4. The long-term mean (thick black contour) and linear trend (shading with thin contour lines) of DJF [u] over 2001–2050: multimodel mean values are shown for (a) CCMVal-2 REF-B1, (b) CCMVal-1, and (c) AR4 models with prescribing ozone recovery. Contour intervals of climatological wind and trend are 10 m s^{-1} starting from 10 m s^{-1} and 0.5 m s^{-1}/decade, respectively. The plot format is the same as Figure 2 of *Son et al.* [2008]. (d, e) Similar to Figures 4a–4c but for the six models which archived both the CCMVal-1 and CCMVal-2 data. Those models are CCSRNIES, CMAM, GEOSCCM, MRI, SOCOL and WACCM. The plot format is the same as Figure 1.

December–January, but it is statistically insignificant. The absence of future trend in tropospheric [*u*] is presumably due to the slow pace of stratospheric O_3 increase (compare Figures 3a and 3d) which would only weakly decelerate the jet and the fact that increase in GHGs continues to accelerate the jet; over this period, GHG and O_3 forcings oppose one another. This result is consistent with previous studies [*Gillett and Thompson*, 2003; *Perlwitz et al.*, 2008; *Son et al.*, 2008, 2009b].

[20] It is noteworthy that the trend shown in Figure 1d is somewhat weaker than the one predicted by the CCMVal-1 models [*Son et al.*, 2008]. Figures 4a–4c show DJF [u] trends for time period of 2001–2050 in three sets of models: the CCMVal-2, CCMVal-1 and AR4 models with prescribing O_3 recovery. Here the latter two are identical to Figures 2a and 2c of *Son et al.* [2008]. The CCMVal-2 models predict a weaker tropospheric [u] trend than the CCMVal-1 models, but one more comparable to the AR4 models with prescribed O_3 recovery. This result suggests that the difference between the CCMVal-1 and AR4 models discussed by *Son et al.* [2008] (Figures 4b and 4c) should not be attributed to interactive stratospheric chemistry (see section 5 for further discussions).

[21] To examine whether the difference between the CCMVal-2 and CCMVal-1 models are significant, multimodel mean trends are separately calculated for those models which archived both the CCMVal-1 and CCMVal-2 data. The near-surface [u] trends are generally not significant except in very narrow regions (Figures 4d and 4e), and the difference between the two sets of CCMVal models is not statistically significant, due to large intermodel variability. Thus Figure 4 cannot be interpreted to show that the CCMVal-2 models unequivocally predict weaker circulation changes than the CCMVal-1 models. It is interesting,

Table 3. Variables Analyzed in The Study[a]

Acronym	Content
$\langle O_3 \rangle_{50}$	Polar cap [O_3] at 50 hPa integrated south of 64°S
$\langle T_P \rangle_{100}$	Polar cap [T] at 100 hPa integrated south of 64°S
$\langle p_{trp} \rangle$	Extratropical zonal mean tropopause pressure integrated south of 50°S
$[u]_{max}$	Jet strength defined by maximum [u] at 850 hPa
$[u]_{lat}$	Jet location defined by location of maximum [u] at 850 hPa
$[H]_{lat}$	Location of the Hadley cell boundary defined by zero [Ψ] at 500 hPa

[a]Here Ψ denotes mass-stream function and angle brackets denote a latitudinal, longitudinal, and seasonal average.

however, that the two sets of models predict quantitatively similar polar cap O_3 trends (not shown), differing more in their tropospheric response.

3.2. SH Circulation Change: Multimodel Mean Trends

[22] The multimodel mean trends are examined for the variables listed in Table 3: polar cap ozone at 50 hPa ($\langle O_3 \rangle_{50}$), polar cap temperature at 100 hPa ($\langle T_P \rangle_{100}$), tropopause pressure in the extratropics ($\langle p_{trp} \rangle$), the location of the tropospheric jet ($[u]_{lat}$), the intensity of the jet ($[u]_{max}$) and the location of the southern boundary of the SH Hadley cell ($[H]_{lat}$). These variables are defined using conventional definitions. The tropopause pressure is identified by the point where the lapse rate reaches 2 K/km temperature [*World Meteorological Organization*, 1957], and the location of the westerly jet is defined by the latitude of maximum [*u*] at 850 hPa [*Lu et al.*, 2008; *Son et al.*, 2009b]. The poleward boundary of the Hadley cell is identified by the zero value of zonal mean mass stream function, [Ψ], at 500 hPa [*Hu and Fu*, 2007; *Lu et al.*, 2008; *Son et al.*, 2009b].

[23] Both the past and future climates are examined using the CCMVal-2 and AR4 model output. Here multimodel mean trends of the AR4 models are calculated separately for models with and without time-varying O_3. This approach is identical to that of *Son et al.* [2009a] except for the analysis period (i.e., 2000–2049 for scenario integrations from *Son et al.* [2009a]) and the latitudinal extent of analysis (i.e., south of 70°S from *Son et al.* [2009a]). Results are summarized in Figure 5 for DJF. Each plot, except Figure 5a, consists of six marks with error bars representing multimodel mean trends and one standard deviation bounds for the six groups of models. From the left to the right, they are derived from the CCMVal-2 REF-B1 integrations (17 models), the AR4 20C3M integrations with O_3 depletion (12 models) and without O_3 depletion (8 models), the AR4 A1B GHGs scenario integrations without O_3 recovery (10 models) and with O_3 recovery (10 models), and the CCMVal-2 REF-B2 integrations (10 models).

[24] Figure 5a shows the stratospheric O_3 trends in the SH late spring. The CCMVal-2 models show significant decrease in stratospheric O_3 in the past (red circle), which is over twice as strong as the increase of O_3 in the future (blue square). Note however that the future trends act over a longer period, so that the total change over the two periods is more comparable. Although direct comparison to observations is not possible due to a lack of observations at a given level for a long-term period, the simulated $\langle O_3 \rangle_{50}$ trend seems to be quite reasonable as can be inferred from their temperature trend, which is quantitatively similar to the observations (Figure 5b). Here we note that the AR4 models show similar temperature trends to the CCMVal2 models, provided only those with time-varying O_3 are considered (grey filled circle and square). Although it is not entirely clear how stratospheric O_3 is prescribed in the AR4 models, this suggests that these two sets of models have comparable O_3 forcing in both the past and future climate integrations.

[25] It is noteworthy in Figure 5b that, in the absence of time-varying O_3, the AR4 models show negligible temperature change in the lower stratosphere not only in the past but also in the future climate integrations (grey open circle and square). Given the fact that anthropogenic GHG increase is stronger in the future than in the past climate integrations, this suggests that GHG increase plays only a minor role in the lower stratospheric temperature change over the pole. We note that the lack of sensitivity to GHG changes between the past and future climate integrations is also found in other variables (grey open circles and squares in Figures 5c–5e) as discussed below.

[26] Figure 5c shows the long-term trend in extratropical tropopause pressure. Lower stratospheric cooling is accompanied by a decrease in tropopause pressure in the extratropics, corresponding to an increase in tropopause height. This sensitivity is anticipated as strong cooling in the lower stratosphere increases the temperature lapse rate near the tropopause, pushing the location where the rate reaches 2 K/km upward [*Santer et al.*, 2003; *Son et al.*, 2009a]. While GHG increase alone tends to cause a continued decrease in tropopause pressure in the 21st century (open square in Figure 5c), this effect is largely canceled by the response to ozone recovery in the future which tends to warm the lower stratosphere and increase tropopause pressure.

[27] Previous studies have shown that decrease in extratropical tropopause pressure (or cooling in the lowermost stratosphere) could cause the westerly jet to move poleward [*Polvani and Kushner*, 2002; *Haigh et al.*, 2005; *Williams*, 2006; *Lorenz and DeWeaver*, 2007]. Consistent results are found in the CCMVal-2 model integrations (Figure 5d). Note that the westerly jet shifts poleward even in the absence of ozone change (grey open circle and square in Figure 5d). This is attributed to increase in GHGs. However, poleward displacement is much stronger in the presence of O_3 depletion and weaker in the presence of O_3 recovery, indicating that stratospheric O_3 plays a significant role in the tropospheric circulation change. A similar sensitivity is also found in the location of the SH summer Hadley cell boundary: stratospheric O_3 depletion tends to strengthen the expansion of the Hadley cell whereas its recovery tends to weaken it (Figure 5e). Although the intermodel differences are quite large, the circulation changes associated with ozone depletion (red circles in Figures 5d and 5e) are still well separated from those associated with ozone recovery (blue squares in Figures 5d and 5e; see also Figure 7c).

[28] It should be noted that the SH summer circulation is not linearly dependent on the magnitude of the GHG forcing. The AR4 models which do not prescribe time-varying O_3 show quantitatively similar trends in the poleward displacement of the jet and expansion of the Hadley cell in both the past and future climate integrations (grey open circle and square in Figures 5d and 5e), despite a faster increase of

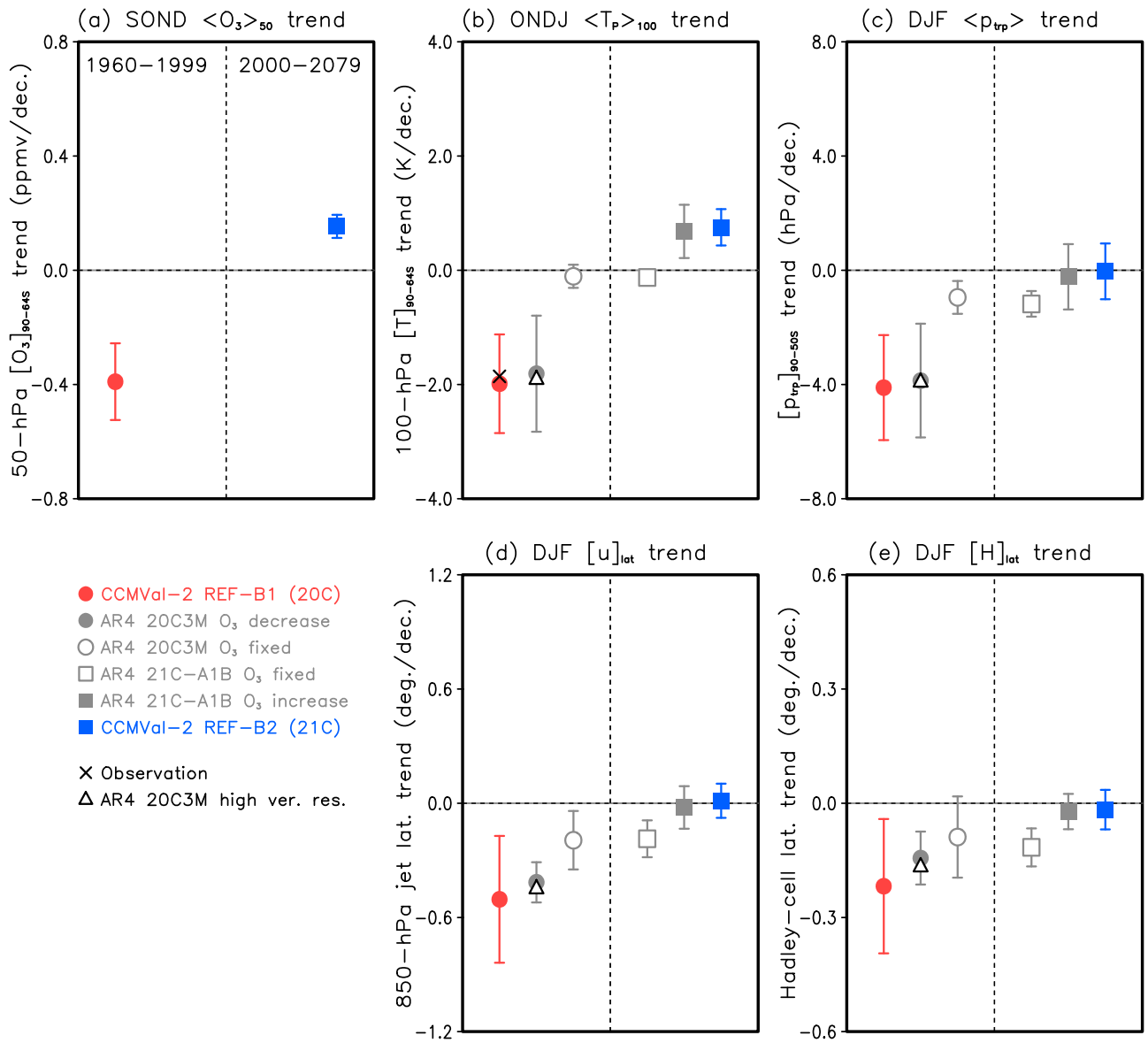

Figure 5. Multimodel mean trends of the SH summer circulation as simulated by the CCMVal-2 and the AR4 models. The mean trends and 1 standard deviation error bars are shown for (a) September–December (SOND) $\langle O_3 \rangle_{50}$, (b) October–January (ONDJ) $\langle T_P \rangle_{100}$, (c) December–February (DJF) $\langle p_{trp} \rangle$, (d) DJF $[u]_{lat}$, and (e) DJF $[H]_{lat}$. See Table 3 for the definition of each variable. In Figure 5a, ozone trends are not shown for the AR4 models with time-varying ozone as they are neither archived nor documented. In Figure 5b the observed temperature trend near 70°S for time period of 1969–1998 [*Thompson and Solomon*, 2002] is shown with a cross for reference. In all plots, multimodel mean trends for the AR4 models with high vertical resolution (models with footnote b in Table 2) are indicated by triangles. Note that negative trends in Figures 5d and 5e denote poleward shift in westerly jet or poleward expansion of the Hadley cell in the SH.

GHG concentration in the future (Although not shown, tropical upper tropospheric warming in the AR4 A1B scenario integrations is about 1.5 times stronger than that in the 20C3M integrations). This puzzling result may be attributed to other external forcings which differ between the past and the future climate. Further studies are needed.

[29] The results presented in Figure 5 suggest that stratospheric ozone influences the entire SH circulation from the stratosphere to the lower troposphere and from the polar regions to the subtropics, as discussed by *Son et al.* [2009b]. Although quantitative differences are present (to be further discussed later), both the CCMVal-2 and the AR4 models show that stratospheric O_3 depletion has helped the SH summer jet to shift poleward and Hadley cell to expand poleward in the recent past. These trends are predicted to be weakened or even disappear in the future due to the anticipated O_3 recovery. To confirm this finding, further analyses are carried out for the SH winter, June–August (JJA), when stratospheric O_3 forcing is essentially absent. As expected,

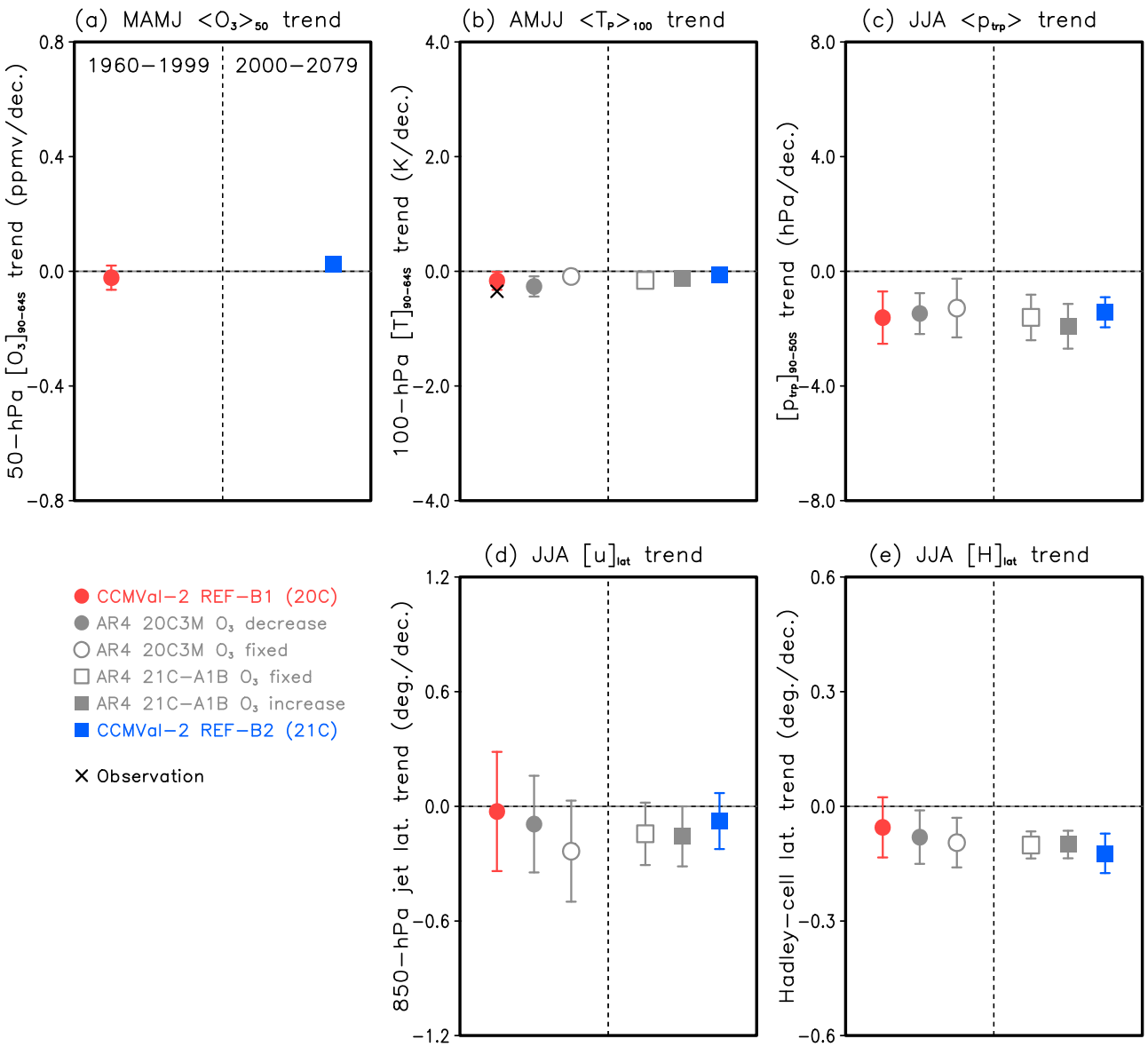

Figure 6. Same as Figure 5 but for (a) March–June (MAMJ), (b) April–July (AMJJ), and (c–e) June–August (JJA).

multimodel mean trends do not show the systematic variation among the six sets of models in that season (Figure 6).

3.3. SH Circulation Change: Individual Model Trends

[30] To quantitatively assess the relationship between stratospheric O_3 and the tropospheric circulation, we analyze the responses of individual models separately. Only the CCMVal-2 models are used here as the AR4 models did not archive O_3 fields. Figure 7a shows the relationship between the September–December (SOND) $\langle O_3 \rangle_{50}$ trend and the October–January (ONDJ) $\langle T_P \rangle_{100}$ trend. These months are chosen to capture the maximum trends of each variable at a given pressure level (see Figure 3). It is found that the ONDJ $\langle T_P \rangle_{100}$ trend is linearly correlated with the SOND $\langle O_3 \rangle_{50}$ trend. The strong correlation is expected because lower stratospheric temperature in the southern high latitudes is largely controlled by radiative processes. Although not shown, a similar linearity, with correlation coefficient of 0.87, is also found between SOND $\langle O_3 \rangle_{50}$ and DJF $\langle p_{trp} \rangle$ trends.

[31] Figure 7b shows the relationship between the SOND $\langle O_3 \rangle_{50}$ and DJF $[u]_{lat}$ trends. Again, a quasi-linear relationship is found, with stronger poleward displacement of the westerly jet associated with stronger O_3 depletion. Although the correlation is weaker for past climate changes, the correlation coefficient (r = 0.55) is still statistically significant and it is remarkably high value considering the fact that $\langle O_3 \rangle_{50}$ is measured at 50 hPa over polar cap and $[u]_{lat}$ is calculated using $[u]$ at 850 hPa in midlatitudes. A similar relationship is also found in DJF $[u]_{max}$ trends: the jet is accelerated much faster when O_3 depletion is stronger. This is expected because poleward displacement of the jet is typically accompanied by intensification of the jet in the SH summer, as shown in Figure 8a (see also Figure 1a).

[32] Figure 7c shows the relationship between SOND $\langle O_3 \rangle_{50}$ and DJF $[H]_{lat}$ trends. A weak quasi-linear relationship

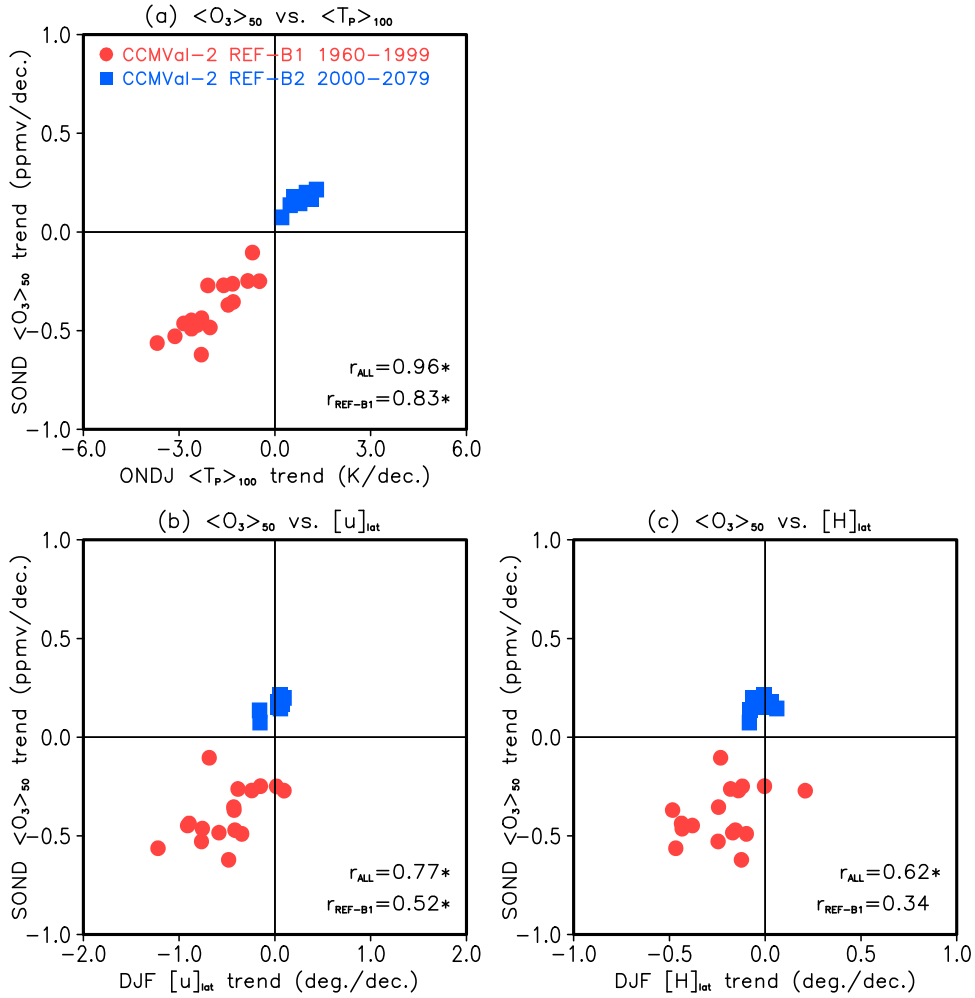

Figure 7. The trend relationship between SOND $\langle O_3 \rangle_{50}$ and several variable of interest for each CCMVal-2 model: (a) ONDJ $\langle T_P \rangle_{100}$, (b) DJF $[u]_{max}$, and (c) DJF $[H]_{lat}$. Linear trends based on the time period of 1960–1999 for the CCMVal-2 REF-B1 runs and 2000–2079 for the CCMVal-2 REF-B2 runs are shown with red circles and blue squares, respectively. Correlation between the two variables is calculated for both all models and only REF-B1 models, and shown in each plot. The correlation coefficients (r) which are statistically significant at the 95% confidence level are indicated with an asterisk.

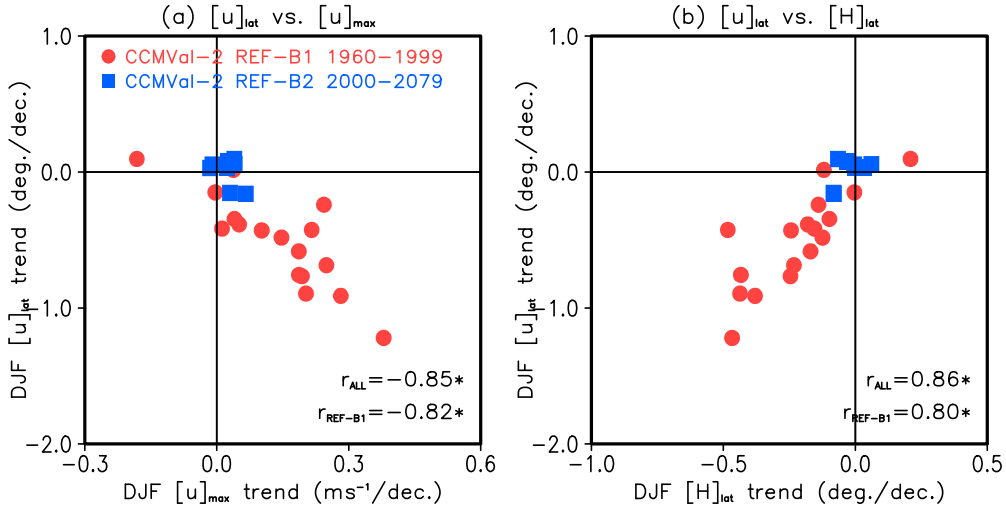

Figure 8. The trend relationships between (a) DJF $[u]_{lat}$ and $[u]_{max}$ and (b) DJF $[u]_{lat}$ and $[H]_{lat}$ in the CCMVal-2 models. The color code is the same as in Figure 7.

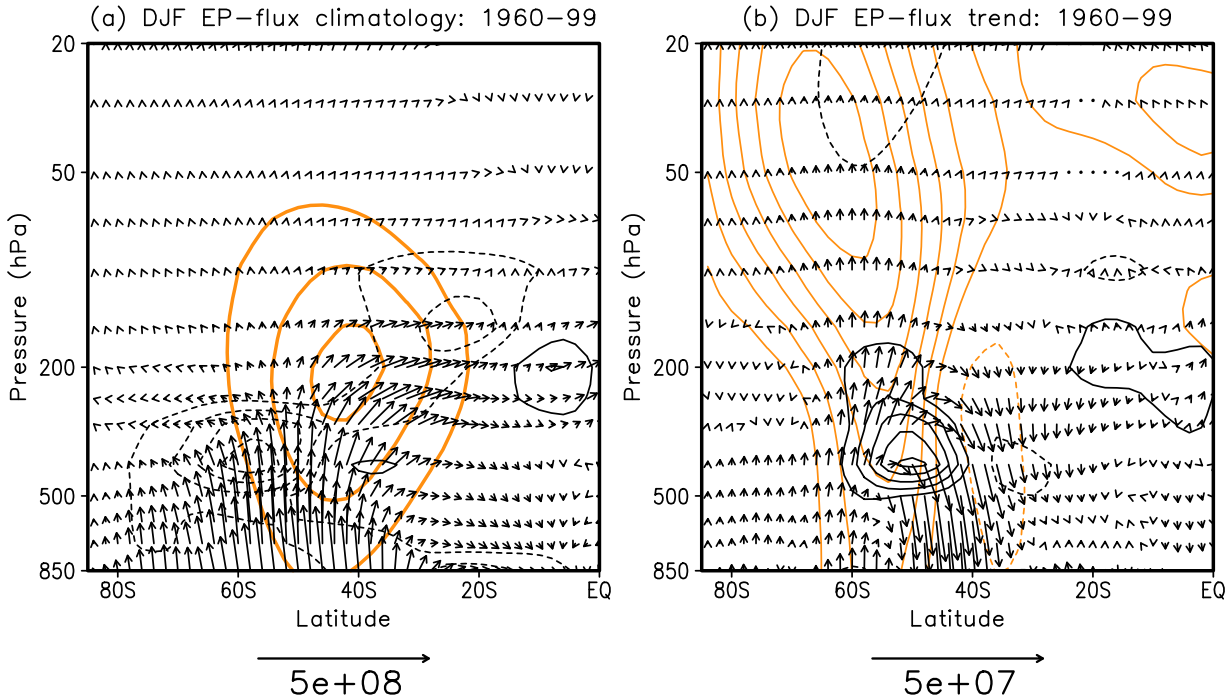

Figure 9. The multimodel mean EP flux vectors and divergence in the SH summer: (a) climatology and (b) linear trend between 1960 and 1999. The vertical component of EP flux vector is multiplied by the aspect ratio, and a reference vector is shown in each plot with units of kg s^{-2} in Figure 9a and kg s^{-2}/decade in Figure 9b. The contour intervals of EP flux divergence are 80 kg m^{-1} s^{-2} in Figure 9a and 4 kg m^{-1} s^{-2}/decade in Figure 9b. The zero lines are omitted. Superimposed orange lines are DJF [*u*] climatology in Figure 9a and multimodel trend in Figure 9b in the same time period. Contour intervals are 10 m s^{-1} and 0.4 m s^{-1}/decade, and the zero lines are omitted. Here multimodel mean values are calculated using the seven CCMVal-2 REF-B1 models which archived zonal mean eddy fields: CMAM, E39CA, GEOSCCM, LMDZrepro, Niwa-SOCOL, SOCOL, and UMUKCA-METO (see Table 1).

is still present, although it is not as strong as for $[u]_{lat}$ trend. It indicates that stratosphere polar cap O_3 affects not only the extratropical circulation but also the subtropical circulation in the SH. This remote influence is partly associated with the fact that the location of the Hadley cell boundary and the location of the jet change coherently in response to external forcing. As shown in Figure 8b, poleward displacement of the jet is typically accompanied by poleward expansion of the Hadley cell in the SH summer. A similar relationship is also found in the AR4 models [*Son et al.*, 2009b].

[33] The systematic circulation changes in response to stratospheric O_3 forcing, for example, stronger poleward displacement and intensification of the jet and stronger poleward expansion of the Hadley cell with stronger O_3 depletion, suggest that tropospheric circulation changes are mediated by the same physical process(es). We argue that circulation changes are highly associated with baroclinic eddies as discussed in previous studies [e.g., *Lu et al.*, 2008]. It is well established that the width of the Hadley cell is strongly influenced by baroclinic eddies [*Held and Phillipps*, 1990; *Kim and Lee*, 2001; *Walker and Schneider*, 2006]. Observations show that the poleward boundary of the Hadley cell is typically located near the zero value of eddy momentum flux convergence (the meridional component of the Eliassen-Palm (EP) flux divergence) in the upper troposphere [e.g., *Son and Lee*, 2005, Figure 1]. It is also known that the extratropical jet, especially the summer hemisphere jet, is largely driven by baroclinic eddies [*Lee and Kim*, 2003] and located at the latitude of maximum eddy momentum flux convergence in the upper troposphere [e.g., *Son and Lee*, 2005, Figure 1]. These suggest that both the jet and the Hadley cell boundary will shift poleward if the eddy fields shift poleward. Figure 9 shows the EP flux climatology and trend over 1960–1999 in the CCMVal-2 REF-B1 model integrations where eddy fields are available. Here the EP flux is calculated using equation (3.5.3) of *Andrews et al.* [1987], based on primitive equations. It confirms that the whole eddy field, as represented by the EP flux, has shifted poleward along with the tropospheric circulation in the last four decades (Figure 9b). Although this analysis does not provide a causal relationship, it suggests that tropospheric changes, driven by stratospheric O_3 loss, are likely mediated by eddies.

4. Possible Mechanisms for O_3-Induced Circulation Change

[34] To better understand the model results, we consider two questions in this section: (1) How does stratospheric ozone influence the tropospheric circulations? (2) Why does the tropospheric response to a given ozone forcing quantitatively differ among the models? Although tropospheric trends are quasi-linearly related with stratospheric O_3 trends, suggesting a common mechanism (question 1), there is sig-

nificant scatter about the linearity in Figure 7. For instance, seven of the models in Figure 7b exhibit $\langle O_3 \rangle_{50}$ trends between −0.4 to −0.5 ppmv/ decade, but $[u]_{lat}$ trends between from −1.0 to −0.2 degrees/decade. We show below that this scatter is not simply due to sampling error.

[35] The above two questions are addressed only qualitatively as the purpose of this section is not to explicitly develop or evaluate dynamical mechanism(s), but rather to briefly review the mechanisms proposed in the literature and examine whether they are consistent with circulation changes simulated by the CCMVal-2 models, and so plausible candidates for explaining the O_3-induced circulation changes in the troposphere. Only the CCMVal-2 REF-B1 integrations are examined since the ozone forcing in the CCMVal-2 REF-B2 integrations is comparatively weaker relative to GHG forcing.

4.1. How Does Stratospheric O_3 Affect the Tropospheric Circulations?

[36] Wave-mean flow interaction theory provides a direct mechanism by which changes in stratospheric wave driving influence the troposphere through the "downward control" [*Haynes et al.*, 1991]. It suggests that wave drag in the stratosphere, which is often quantified by EP flux divergence, can influence the troposphere by modifying the mean meridional circulation via geostrophic and hydrostatic balances. A series of modeling studies [*Kushner and Polvani*, 2004; *Song and Robinson*, 2004], however, have cast doubt on its role, as downward control fails to explain the stratosphere-troposphere coupling in highly controlled, relatively simple model integrations.

[37] To explore downward control with the CCMVal-2 data set, we examine whether the quasi-barotropic acceleration of the SH jet in association with O_3 depletion (Figure 1a) is consistent with the downward control argument. Figure 9b shows the multimodel mean trend of the EP flux in the CCMVal-2 REF-B1 integrations. The EP flux divergence does exhibit a negative trend around 20 hPa and 60°S. Although weak, this negative trend is statistically significant. The resulting mean meridional circulation computed from downward control, however, would drive surface easterlies instead of westerlies, suggesting that downward control is not likely relevant to O_3-induced surface wind change in the CCMVal-2 model integrations.

[38] Other studies have considered the influence of the lower stratospheric wind on tropospheric baroclinic eddies [*Charlton et al.*, 2004; *Kushner and Polvani*, 2004; *Song and Robinson*, 2004]. *Chen and Held* [2007] suggest that O_3-induced zonal wind change in the lower stratosphere may modify tropospheric eddies by changing the phase speed of baroclinic waves in the troposphere. Unfortunately this mechanism cannot be evaluated with the monthly mean zonally averaged fields used in this study. Based on quasi-geostrophic refractive index dynamics, *Simpson et al.* [2009] proposed that lower stratospheric thermal forcing might communicate with the troposphere by changing the potential vorticity gradient, which alters the propagation direction of baroclinic waves. Although this is consistent with the EP flux trends shown in Figure 9b, it is unclear whether changes in wave propagation in the CCMVal-2 models, e.g., the EP flux change in Figure 9b, are the response to stratospheric forcing or the response to tropospheric circulation change itself.

[39] As an alternative mechanism, *Grise et al.* [2009] argued that observed circulation change in the SH might partly result from radiative cooling in the troposphere caused by ozone loss; lower stratospheric cooling could reduce long-wave radiation from the stratosphere to the troposphere. It leads to a significant cooling in the extratropical troposphere which in turn modifies the tropospheric circulation. This argument, however, is unlikely to apply to the CCMVal-2 models as the polar cap temperature trend is almost negligible in the troposphere (Figure 3b).

[40] In summary there is, at present, no conclusive mechanism on how stratospheric O_3 influences the troposphere, although downward control and long-wave radiation arguments do not likely hold. It calls for more extensive study. Particularly, the possible role of nonlinear wave-mean flow interaction deserves detailed investigation. Recent studies by *Wittman et al.* [2007] and *Kunz et al.* [2009] have shown that the linear theory, which is the basis of work by *Chen and Held* [2007] and *Simpson et al.* [2009], cannot explain the spatial structure of wave breaking caused by the stratospheric wind.

4.2. What Controls the Amplitude of the Tropospheric Response to O_3 Depletion?

[41] We next examine the intermodel difference in tropospheric circulation sensitivity to O_3, in particular the spread around the quasi-linear relationship illustrated in Figure 7. This scatter is unlikely to be the result of sampling errors or differences in their external forcing, since trends are calculated with 4 decade long time series and all models are driven by identical forcings. Among many possible reasons, we show below that it is partly associated with the model climatology, which differs substantially from one model to another (Figures 2a and 2c).

[42] The relationship between the climatological jet location at 850 hPa and $[u]_{max}$ trend normalized by $\langle O_3 \rangle_{50}$ trend is presented in Figure 10a. The normalized $[u]_{max}$ trend is somewhat linearly correlated with model climatology; that is, circulation responses to O_3 changes are generally stronger in models where the climatological jet is located in lower latitudes. This appears counterintuitive at first, as ozone forcing is better separated from the jet as the jet is located in lower latitudes. A similar relationship between climatology and climate response to external forcing, however, has also been identified for different external forcings in both idealized [*Simpson et al.*, 2010] and comprehensive GCMs [*Kidston and Gerber*, 2010].

[43] The dependency of ozone-induced circulation changes on model climatology is perhaps not surprising. *Son and Lee* [2006] have shown that the projection of climate change onto the annular mode (e.g., Figure 1a) is strongly dependent on the structure of time-mean flow. *Gerber and Polvani* [2009] and *Chan and Plumb* [2009] have also shown that the stratospheric influence on the tropospheric circulation is highly sensitive to the background flow in the troposphere. Although a detailed investigation is beyond the scope of the present study, we address below two possible scenarios that might explain this sensitivity: a simple geometric constraint and a dynamical constraint.

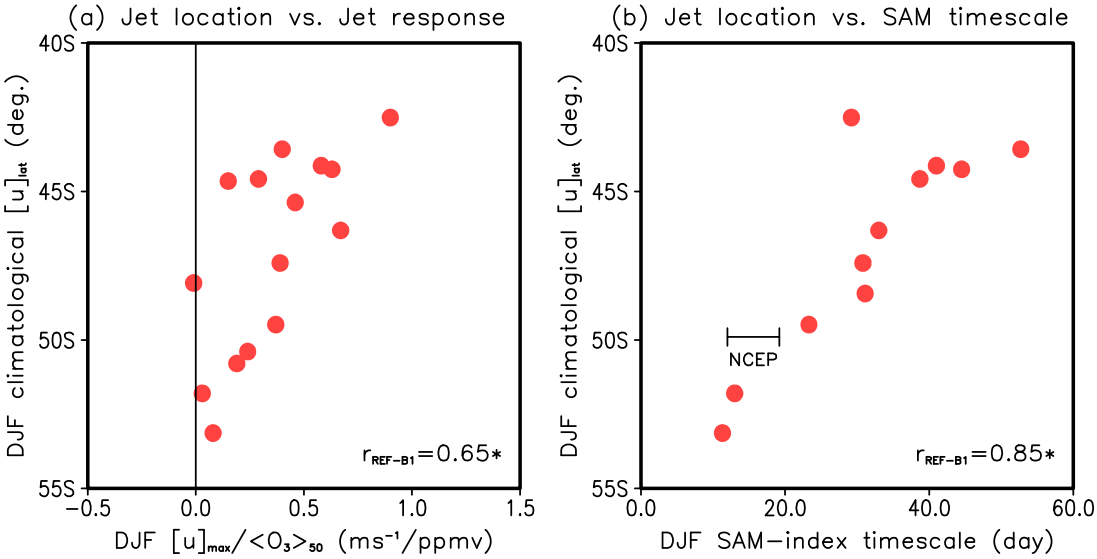

Figure 10. The relationship between the climatological jet location in the CCMVal-2 REF-B1 scenario and (a) the tropospheric jet response to ozone depletion and (b) time scale of the SAM index in the SH summer as simulated by the CCMVal-2 REF-B1 models. In Figure 10a the tropospheric $[u]_{max}$ trend is normalized by the $\langle O_3 \rangle_{50}$ trend. Only 15 models are used here excluding two outliers which show too weak $\langle O_3 \rangle_{50}$ trend or negative $[u]_{max}$ trend (see Figures 7 and 8). In Figure 10b, only 11 models are used, as others have not archived sufficiently daily data. Time scale based on the NCEP-NCAR reanalysis [*Baldwin et al.*, 2003] is indicated with error bar in Figure 10b.

[44] The geometry of the sphere and the equator-to-pole temperature difference establish a high-latitude limit to the extent of the extratropical jet. If the jet changes its location in response to external forcing, the poleward displacement (and intensification) may preferentially occur when the climatological jet is located in the latitudes lower than this high-latitude limit. In models where the climatological jet is located in high latitudes, it is likely difficult to move the jet farther poleward. In contrast, in models where the climatological jet exhibits an equatorward bias, there is much more room for the jet to move poleward. This simple, likely oversimplified, argument amounts to a geometric constraint.

[45] The dynamic constraint is linked to a connection between internal variability and background flow. A series of idealized modeling studies by *Gerber and Vallis* [2007], *Son et al.* [2008] and *Simpson et al.* [2010] have shown that the e-folding time scale of zonal mean flow variability or annular mode (hereafter simply "the time scale") is highly sensitive to the background flow. They found that it is shorter in integrations where the climatological eddy-driven jet is located in higher latitudes. Figure 10b shows the relationship between the time scale and the location of climatological jet for the CCMVal-2 models. Here, the time scale is estimated by e-folding time scale of the SAM index, derived from the Empirical Orthogonal Function (EOF) analyses of daily zonal mean geopotential height. This e-folding time scale is first calculated at each model level and then integrated from the surface to 250 hPa. (See *Gerber et al.* [2010] for further details.) It is found that the time scale is highly correlated with the location of climatological jet, decreasing as the jet is located in higher latitudes. This is consistent with idealized model experiments. A similar relationship is also found in the AR4 model integrations [*Kidston and Gerber*, 2010].

[46] The fluctuation-dissipation theorem links the internal variability of a system to its response to external forcing [e.g., *Leith*, 1975]. Proper application of fluctuation-dissipation theory requires knowledge of the correlation structure between all modes of the system, or at least a subset sufficient to represent the dynamics [e.g., *Majda et al.*, 2010], but such an analysis is beyond the scope of this study. As discussed by *Leith* [1975], however, a simpler relationship may apply if the annular mode is sufficiently uncorrelated with other modes in the system. In this case one might expect that for models with more persistent internal variability (e.g., longer time scale), the jet should respond more to external forcing, as found by *Gerber et al.* [2008] and *Ring and Plumb* [2008] in idealized model integrations. This is to a large degree in agreement with the findings of Figure 10.

[47] Why is the e-folding time scale shorter as the jet is located in higher latitudes? It may arise from meridional propagation of baroclinic eddies [*Son et al.*, 2007; *Simpson et al.*, 2010]. The summer hemisphere jet is essentially driven by eddies and generally forms at the region of maximum baroclinicity as discussed in section 3.3 (see also Figure 9a). Given that baroclinicity in the subtropics is fixed by the Hadley circulation, the extratropical jet at higher latitudes implies a broader baroclinic zone where baroclinic waves can propagate. This may allow eddies to propagate latitudinally more effectively, weakening the stability of the eddy fluxes which maintain the zonal mean flow anomalies. The result would be a less stationary zonal mean flow anomaly in time, leading to shorter time scale. The opposite would be the case for the jet located in lower latitudes. Eddy activity would be confined to a more limited latitude band, and would increase the chances that eddy fluxes continuously occur at similar latitudes, making zonal mean

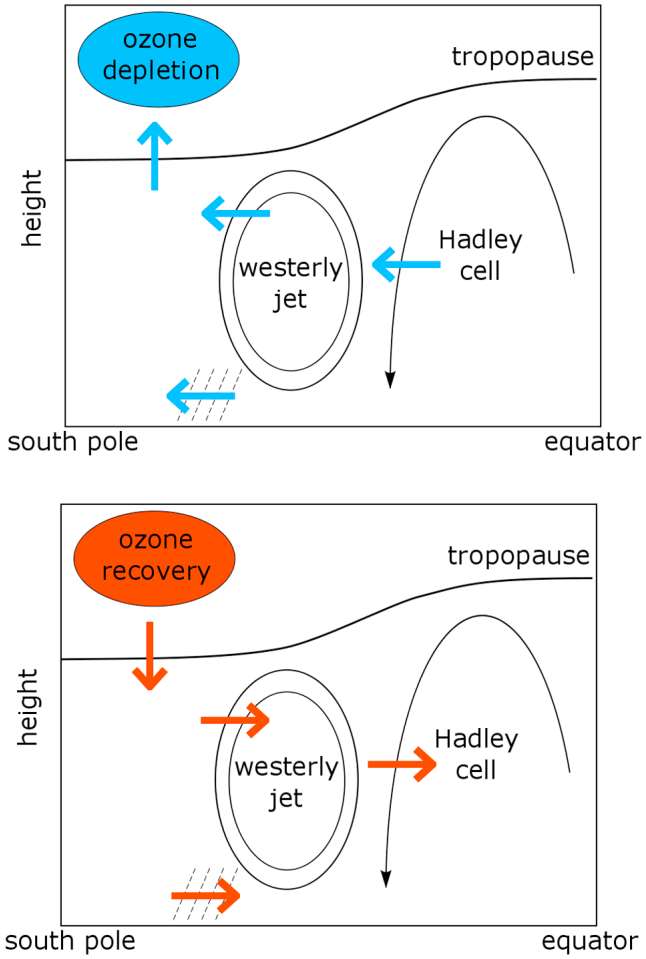

Figure 11. A schematic representation of the impact of stratospheric ozone loss and recovery on the tropospheric circulation in the SH summer. Changes in the extratropical tropopause height and location of the westerly jet, storm track (and associated midlatitude precipitation), and the poleward boundary of the Hadley cell are highlighted.

flow anomalies persist longer. See *Gerber and Vallis* [2007], *Son et al.* [2007], and *Simpson et al.* [2010] for further discussion.

5. Summary and Discussion

[48] Our analyses of both CCMVal-2 and AR4 model integrations confirm the growing body of evidence that stratospheric O_3 plays a significant role in the tropospheric circulation of the SH in austral summer [e.g., *Thompson and Solomon*, 2002; *Gillett and Thompson*, 2003; *Shindell and Schmidt*, 2004; *Arblaster and Meehl*, 2006; *Miller et al.*, 2006; *Cai and Cowan*, 2007; *Perlwitz et al.*, 2008; *Son et al.*, 2008, 2009b, 2009a]. Its impacts are illustrated schematically in Figure 11. Stratospheric O_3 depletion has (1) decreased the lower stratospheric temperature, (2) increased the tropopause height, (3) intensified the westerly jet and (4) displaced it poleward, and (5) expanded the Hadley cell poleward (Figure 11a). The opposite is expected when stratospheric O_3 increases, as predicted to occur over the next several decades (Figure 11b). Since circulation changes driven by O_3 recovery would oppose those by tropospheric GHGs increase, it is anticipated that tropospheric circulation changes in the future will be substantially weaker than, or even the reverse of, those observed in the past. All of these are consistent with previous studies.

[49] Although not the focus of this study, stratospheric O_3 is known to affect the surface climate [e.g., *Thompson and Solomon*, 2002; *Son et al.*, 2009a]. *Thompson and Solomon* [2002] have shown that stratospheric O_3 depletion has warmed the Antarctic peninsula, but cooled the Antarctic continent in the recent past. It has also contributed to a dipolar change of sea level pressure between midlatitude and subpolar regions, equivalent to strengthening of positive trend in the SAM index. The resulting enhancement of pressure gradient accompanies strong surface westerly around 60°S, consistent with quasi-barotropic acceleration of zonal wind shown in Figure 1a. As noted by *Son et al.* [2009a], stratospheric O_3 also influences global hydrology. Expansion of the subtropical dry zone in the recent past is strongly associated with poleward expansion of the Hadley cell [*Lu et al.*, 2007]. Likewise, the poleward shift of the extratropical storm tracks is largely accompanied by poleward displacement of westerly jet as indicated in Figure 11 [e.g., *Yin*, 2005]. We expect that these direct and indirect impacts of O_3 will reverse in the future due to the anticipated recovery of stratospheric O_3.

[50] The changes in surface climate, partly associated with stratospheric O_3, are also known to affect the upper ocean salinity and temperature. Observational studies have shown that the upper ocean in the southern high latitudes has been freshening over the last 4 decades [*Gille*, 2002; *Böning et al.*, 2008]. This has been attributed in part to the enhanced precipitation over the Southern Ocean resulting from the poleward shift of the tropospheric circulation [*Böning et al.*, 2008]. It has also been suggested that the upper ocean temperature might be modulated by surface wind change (e.g., Figure 1a) through Ekman transport [e.g., *Fyfe et al.*, 1999]. These changes in the upper ocean in turn feedback on the troposphere, possibly amplifying the O_3-induced circulation change in the SH.

[51] The potential links between stratospheric O_3 and the ocean suggest that climate prediction in the SH may require coupling from top to bottom, with models which incorporate both stratospheric chemistry and an interactive ocean. The computational expense to resolve both stratospheric chemistry and the ocean circulation has limited such modeling at present. This raises a practical question: can coupled models such as those participating in the IPCC AR4 produce the correct climate response, given a reasonable O_3 forcing? An ideal approach to answer the question is to compare identical model integrations with interactive O_3 or prescribed O_3, as in work by *Gillett et al.* [2009] and *Waugh et al.* [2009]. An imperfect alternative, but one that allows us to incorporate all models, is to directly compare CCMVal-2 model predictions with the AR4 model predictions that were forced with O_3 loss and recovery. Figure 5b shows that the AR4 models with time-varying O_3 have quantitatively similar temperature trends to the CCMVal-2 models, indicating that the two sets of models have comparable O_3 forcings. The resulting circulation changes in the troposphere are also comparable (Figures 5d and 5e), suggesting that interactive O_3 may not be necessary if O_3 is reasonably prescribed in

the AR4-type coupled models. In this regard, a potentially important result of this study is the closer agreement on future circulation trends between CCMVal-2 and AR4 models (Figure 4), as compared with the differences between CCMVal-1 and AR4 models found by *Son et al.* [2008].

[52] We note, however, that the circulation changes predicted by the AR4 models are somewhat weaker than those predicted by the CCMVal-2 models in the past climate integrations. The difference is not statistically significant, and so could be associated with sampling errors, but there may be physical reasons for the decreased sensitivity in the AR4 models. The underestimate could be associated with vertical resolution in the stratosphere, which is coarse in many AR4 models. *Karpechko et al.* [2008] found that relatively high vertical resolution is required to capture ozone-induced polar cap temperature change. The multimodel mean trends based on models with reasonably high vertical resolution in the stratosphere are indeed stronger (triangles in Figure 5), but they are still weaker than those in the CCMVal-2 models. Another possibility is the deficiency in the prescription of ozone forcing itself [*Gillett et al.*, 2009; *Waugh et al.*, 2009]. Stratospheric O_3 forcing in most AR4 models is zonally symmetric, in contrast with observations and CCMVal-2 model output, which exhibit strong asymmetries. The differences between the CCMVal-2 models and the AR4 models shown in Figures 5d and 5e, are in fact comparable to those found by *Waugh et al.* [2009], who compared model integrations with fully interactive ozone and those with zonally averaged ozone forcing.

[53] Lastly, our investigation of intermodel differences in the quantitative response of the troposphere to stratospheric ozone highlights the importance of model climatology and large-scale dynamics. The location of the SH jet, a key element of the climatology particularly for interaction with the ocean, varies by over 10° across the CCMVal-2 models, and most models exhibit an equatorward bias relative to observations. While errors in the climatology have consequences for regional climate in their own right, these biases also appear to be closely related with differences in time scales of internal variability and differences in tropospheric response to stratospheric O_3 change among the models. It suggests that uncertainty in large-scale dynamics must be addressed alongside the processes governing the coupling between chemistry and climate.

[54] **Acknowledgments.** Helpful comments by Petra Huck and three anonymous reviewers are gratefully appreciated. The authors thank the Program for Climate Model Diagnosis and Intercomparison (PCMDI) for collecting and archiving the CMIP3 model data, the JSC/CLIVAR Working Groups on Coupled Modeling (WGCM) and their Coupled Model Intercomparison Project (CMIP) and Climate Simulation Panel for organizing the model data analysis activity, and the IPCC WG1 TSU for technical support. The IPCC Data Archive at Lawrence Livermore National Laboratory is supported by the Office of Sciences, U.S. Department of Energy. We also thank all of the modeling groups for making their simulations available for this analysis, the second round of the Chemistry-Climate Model Validation (CCMVal-2) Activity for WCRP (World Climate Research Programme) SPARC (Stratospheric Processes and their Role in Climate) project for organizing and coordinating the model data analysis activity, and the British Atmospheric Data Center (BADC) for collecting and archiving the CCMVal-2 model output. The work of S.W.S. is supported by NSERC discovery grant. E.P.G. and L.M.P. are supported by grants from the US NSF to New York University and Columbia University, respectively. K.H.S. and S.W.S. were funded by the KMA R&D program under grant RACS 2010–2017. D.W. is partly supported by U.S. NSF. N.B. and S.H. are supported by the Joint DECC and Defra Integrated Climate Programme, DECC/Defra (GA01101). The CCSRNIES research was supported by the Global Environmental Research Found of the Ministry of the Environment of Japan (A-071), and the simulations were completed with the supercomputer at CGER, NIES, Japan. The MRI simulation was made with the supercomputer at the NIES, Japan. The scientific work of the European CCM groups was supported by the European Commission through the project SCOUT-O3 under the 6th Framework Programme. The National Center for Atmospheric Research is operated by the University Corporation for Atmospheric Research under sponsorship of the National Science Foundation. Any opinions, findings, and conclusions or recommendations expressed in the publication are those of the authors and do not necessarily reflect the views of the National Science Foundation.

References

Akiyoshi, H., L. B. Zhou, Y. Yamashita, K. Sakamoto, M. Yoshiki, T. Nagashima, M. Takahashi, J. Kurokawa, M. Takigawa, and T. Imamura (2009), A CCM simulation of the breakup of the antarctic polar vortex in the years 1980–2004 under the CCMVal scenarios, *J. Geophys. Res.*, *114*, D03103, doi:10.1029/2007JD009261.

Andrews, D. G., J. R. Holton, and C. B. Leovy (1987), *Middle Atmosphere Dynamics*, 489 pp., Academic, San Diego, Calif.

Arblaster, J. M., and G. A. Meehl (2006), Contribution of external forcings to southern annular mode trends, *J. Clim.*, *19*, 2896–2905.

Austin, J., and N. Butchart (2003), Coupled chemistry-climate model simulation for the period 1980 to 2020: Ozone depletion and the start of ozone recovery, *Q. J. R. Meteorol. Soc.*, *129*, 3225–3249.

Austin, J., and R. J. Wilson (2010), Sensitivity of polar ozone to sea surface temperatures and halogen amounts, *J. Geophys. Res.*, *115*, D18303, doi:10.1029/2009JD013292.

Austin, J., et al. (2010), Decline and recovery of total column ozone using a multimodel time series analysis, *J. Geophys. Res.*, doi:10.1029/2010JD013857, in press.

Baldwin, M. P., D. B. Stephenson, D. W. J. Thompson, T. J. Dunkerton, A. J. Charlton, and A. O'Neill (2003), Stratospheric memory and skill of extended-range weather forecasts, *Science*, *301*, 636–640.

Bengtsson, L., K. I. Hodges, and E. Roeckner (2006), Storm tracks and climate change, *J. Clim.*, *19*, 3518–3543.

Böning, C. W., A. Dispert, M. Visbeck, S. R. Rintoul, and F. U. Schwarzkopf (2008), The response of the antarctic circumpolar current to recent climate change, *Nat. Geosci.*, *1*, 864–869.

Cai, W., and T. Cowan (2007), Trends in Southern Hemisphere circulation in IPCC AR4 models over 1950–99: Ozone depletion versus greenhouse forcing, *J. Clim.*, *20*, 681–693.

Chan, C. J., and R. A. Plumb (2009), The response to stratospheric forcing and its dependence on the state of the troposphere, *J. Atmos. Sci.*, *66*, 2107–2115.

Charlton, A. J., A. O'Neill, W. Lahoz, and A. Massacand (2004), Sensitivity of tropospheric forecasts to stratospheric initial conditions, *Q. J. R. Meteorol. Soc.*, *130*, 1771–1792.

Chen, G., and I. M. Held (2007), Phase speed spectra and the recent poleward shift of Southern Hemisphere surface westerlies, *Geophys. Res. Lett.*, *34*, L21805, doi:10.1029/2007GL031200.

Cordero, E. C., and P. M. de F. Forster (2006), Stratospheric variability and trends in models used for the IPCC AR4, *Atmos. Chem. Phys.*, *6*, 5369–5380.

de Grandpré, J., S. R. Beagley, V. I. Fomichev, E. Griffioen, J. C. McConnell, A. S. Medvedev, and T. G. Shepherd (2000), Ozone climatology using interactive chemistry: Results from the Canadian middle atmosphere model, *J. Geophys. Res.*, *105*, 26,475–26,491.

Déqué, M. (2007), Frequency of precipitation and temperature extremes over France in an anthropogenic scenario: Model results and statistical correction accoring to observed values, *Global Planet. Change*, *57*, 16–26.

Egorova, T., E. Rozanov, V. Zubov, E. Manzini, W. Schmutz, and T. Peter (2005), Chemistry climate model SOCOL: A validation of the present-day climatology, *Atmos. Chem. Phys.*, *5*, 1557–1576.

Eyring, V., M. P. Chipperfield, M. A. Giorgetta, D. E. Kinnison, K. Matthes, P. A. Newman, S. Pawson, T. G. Shepherd, and D. W. Waugh (2008), Overview of the new CCMval reference and sensitivity simulations in support of upcoming ozone and climate assessments and the planned SPARC CCMVal report, *SPARC Newsl.*, *30*, 20–26.

Fogt, R. L., J. Perlwitz, A. J. Monaghan, D. H. Bromwich, J. M. Jones, and G. J. Marshall (2009), Historical SAM variability. Part II: twentieth-

century variability and trends from reconstructions, observations, and the IPCC AR4 models, *J. Clim.*, *22*, 5346–5365.

Frierson, D. M. W., J. Lu, and G. Chen (2007), Width of the Hadley cell in simple and comprehensive general circulation models, *Geophys. Res. Lett.*, *34*, L18804, doi:10.1029/2007GL031115.

Fu, Q., C. Johanson, C. M. Wallace, and T. Reichler (2006), Enhanced mid-latiude tropospheric warming in satellite measurements, *Science*, *312*, 1179.

Fyfe, J. C., O. A. Saenko, K. Zickfeld, M. Eby, and A. J. Weaver (1999), The Arctic and Antarctic oscillations and their projected changes under global warming, *Geophys. Res. Lett.*, *26*, 1601–1604.

Fyfe, J. C., G. Boer, and G. Flato (2007), The role of poleward-intensifying winds on Southern Ocean warming, *J. Clim.*, *20*, 5391–5400.

Garcia, R. R., D. R. Marsh, D. E. Kinnison, B. A. Boville, and F. Sassi (2007), Simulation of secular trends in the middle atmosphere, 1950–2003, *J. Geophys. Res.*, *112*, D09301, doi:10.1029/2006JD007485.

Garny, H., M. Dameris, and A. Stenke (2009), Impact of prescribed SSTs on climatologies and long-term trends in CCM simulations, *Atmos. Chem. Phys.*, *9*, 6017–6031.

Gerber, E. P., and L. M. Polvani (2009), Stratosphere-troposphere coupling in a relatively simple AGCM: The importance of stratospheric variability, *J. Clim.*, *22*, 1920–1933.

Gerber, E. P., and G. K. Vallis (2007), Eddy-zonal flow interactions and the persistence of the zonal index, *J. Atmos. Sci.*, *64*, 3296–3311.

Gerber, E. P., S. Voronin, and L. M. Polvani (2008), Testing the annular mode autocorrelation time scale in simple atmospheric general circulation models, *Mon. Weather Rev.*, *136*, 1523–1536.

Gerber, E. P., et al. (2010), Stratosphere-troposphere coupling and annular mode variability in chemistry-climate models, *J. Geophys. Res.*, *115*, D00M06, doi:10.1029/2009JD013770.

Gille, S. T. (2002), Warming of the Southern Ocean since the 1950s, *Science*, *295*, 1275–1277.

Gillett, N. P., and D. W. J. Thompson (2003), Simulation of recent Southern Hemisphere climate change, *Science*, *302*, 273–275.

Gillett, N. P., J. F. Scinocca, D. A. Plummer, and M. C. Reader (2009), Sensitivity of climate to dynamically-consistent zonal asymmetries in ozone, *Geophys. Res. Lett.*, *36*, L10809, doi:10.1029/2009GL037246.

Grise, K. M., D. W. J. Thompson, and P. M. Forster (2009), On the role of radiative processes in stratosphere-troposphere coupling, *J. Clim.*, pp. 4154–4161, doi:10.1175/2009JCLI2756.1.

Haigh, J. D., M. Blackburn, and R. Day (2005), The response of tropospheric circulation to perturbations in lower-stratospheric temperature, *J. Clim.*, *18*, 3672–3685.

Haynes, P. H., M. E. McIntyre, T. G. Shepherd, C. J. Marks, and K. P. Shine (1991), One the downward control of extratropical diabatic circulations by eddy-induced mean zonal forces, *J. Atmos. Sci.*, *48*, 651–678.

Held, I., and P. Phillipps (1990), A barotropic model of the interaction between the Hadley cell and a Rossby wave, *J. Atmos. Sci.*, *47*, 856–869.

Hu, Y., and Q. Fu (2007), Observed poleward expansion of the Hadley circulation since 1979, *Atmos. Chem. Phys.*, *7*, 5229–5236.

Jöckel, P., et al. (2006), The atmospheric chemistry general circulation model ECHAM/MESSy1: Consistent simulation of ozone from the surface to the mesosphere, *Atmos. Chem. Phys.*, *6*, 5067–5104.

Johanson, C. M., and Q. Fu (2009), Hadley cell widening: Model simulations versus observations, *J. Clim.*, *22*, 2713–2725.

Jourdain, L., S. Bekki, F. Lott, and F. Lefèvre (2008), The coupled chemistry model LMDz reprobus: Description of a transient simulation of the period 1980–1999, *Ann. Geophys.*, *26*, 1391–1413.

Kalnay, E., et al. (1996), The NCEP/NCAR 40-year reanalysis project, *Bull. Am. Meteorol. Soc.*, *77*, 437–471.

Karpechko, A. Y., N. P. Gillett, G. J. Marshall, and A. A. Scaife (2008), Stratospheric influence on circulation changes in the Southern Hemisphere troposphere in coupled models, *Geophys. Res. Lett.*, *35*, L20806, doi:10.1029/2008GL035354.

Kidston, J., and E. P. Gerber (2010), Intermodel variability of the poleward shift of the austral jet stream in the CMIP3 integrations linked to biases in 20th century climatology, *Geophys. Res. Lett.*, *37*, L09708, doi:10.1029/2010GL042873.

Kim, H.-K., and S. Lee (2001), Hadley cell dynamics in a primitive equation model. Part II: Nonaxisymmetric flow, *J. Atmos. Sci.*, *58*, 2859–2871.

Kunz, T., K. Fraedrich, and F. Lunkeit (2009), Response of idealized baroclinic wave life cycles to stratospheric flow conditions, *J. Atmos. Sci.*, *66*, 2288–2302.

Kushner, P. J., and L. M. Polvani (2004), Stratosphere-troposphere coupling in a relatively simple AGCM: The role of eddies, *J. Clim.*, *17*, 629–639.

Kushner, P. J., I. M. Held, and T. L. Delworth (2001), Southern Hemisphere atmospheric circulation response to global warming, *J. Clim.*, *14*, 2238–2249.

Lamarque, J. F., D. E. Kinnison, P. G. Hess, and F. M. Vitt (2008), Simulated lower stratospheric trends between 1970 and 2005: Identifying the role of climate and composition changes, *J. Geophys. Res.*, *113*, D12301, doi:10.1029/2007JD009277.

Lee, S., and H.-K. Kim (2003), The dynamical relationship between subtropical and eddy-driven jets, *J. Atmos. Sci.*, *60*, 1490–1503.

Leith, C. E. (1975), Climate response and fluctuation dissipation, *J. Atmos. Sci.*, *32*, 2022–2026.

Lorenz, D. J., and E. T. DeWeaver (2007), Tropopause height and zonal wind response to global warming in the IPCC scenario integrations, *J. Geophys. Res.*, *112*, D10119, doi:10.1029/2006JD008087.

Lu, J., G. Vecchi, and T. Reichler (2007), Expansion of the Hadley cell under global warming, *Geophys. Res. Lett.*, *34*, L06805, doi:10.1029/2006GL028443.

Lu, J., G. Chen, and D. M. W. Frierson (2008), Response of the zonal mean atmospheric circulation to El Niño versus global warming, *J. Clim.*, *22*, 5835–5851.

Majda, A. J., B. Gershgorin, and Y. Yuan (2010), Low frequency climate response and fluctuation-dissipation theorems: Theory and practice, *J. Atmos. Sci.*, *67*, 1186–1201, doi:10.1175/2009JAS3264.1.

Marshall, G. J. (2003), Trends in the southern annular mode from observations and reanalyses, *J. Clim.*, *16*, 4134–4143.

Miller, R. L., G. A. Schmidt, and D. T. Shindell (2006), Forced annular variations in the 20th century Intergovermental Panel on Climate Change Fourth Assessment Report models, *J. Geophys. Res.*, *111*, D18101, doi:10.1029/2005JD006323.

Morgenstern, O., P. Braesicke, M. M. Hurwitz, F. M. O'Connor, A. C. Bushell, C. E. Johnson, and J. A. Pyle (2008), The world avoided by the Montreal Protocol, *Geophys. Res. Lett.*, *35*, L16811, doi:10.1029/2008GL034590.

Morgenstern, O., P. Braesicke, F. M. O'Connor, A. C. Bushell, C. E. Johnson, S. M. Osprey, and J. A. Pyle (2009), Evaluation of the new UKCA climate-composition model. Part 1: The stratosphere, *Geosci. Model Dev.*, *1*, 43–57.

Morgenstern, O., et al. (2010), Review of the formulation of present-generation stratospheric chemistry-climate models and associated external forcings, *J. Geophys. Res.*, *115*, D00M02, doi:10.1029/2009JD013728.

Pawson, S., R. S. Stolarski, A. R. Douglass, P. A. Newman, J. E. Nielsen, S. M. Frith, and M. L. Gupta (2008), Goddard Earth Observing System chemistry-climate model simulations of stratospheric ozone-temperature coupling between 1950 and 2005, *J. Geophys. Res.*, *113*, D12103, doi:10.1029/2007JD009511.

Perlwitz, J., S. Pawson, R. L. Fogt, J. E. Nielsen, and W. D. Neff (2008), Impact of stratospheric ozone hole recovery on Antarctic climate, *Geophys. Res. Lett.*, *35*, L08714, doi:10.1029/2008GL033317.

Polvani, L. M., and P. J. Kushner (2002), Tropospheric response to stratospheric perturbations in a relatively simple general circulation model, *Geophys. Res. Lett.*, *29*(7), 1114, doi:10.1029/2001GL014284.

Polvani, L. M., D. W. Waugh, G. J. P. Correa, and S.-W. Son (2010), Stratospheric ozone depletion: The main driver of 20th century atmospheric circulation changes in the Southern Hemisphere, *J. Clim.*, in press.

Randall, D. A., et al. (2007), Climate models and their evaluation, in *Climate Change 2007: The Physical Sciences Basis. Contribution of Working Group I to the Fourth Assessment Report of the Intergovernmental Panel on Climate Change*, edited by S. Solomon et al., Cambridge Univ. Press, Cambridge, U. K.

Randel, W. J., and F. Wu (1999), A stratospheric ozone trends data set for global modeling studies, *Geophys. Res. Lett.*, *26*, 3089–3092.

Ring, M. J., and R. A. Plumb (2008), The response of a simplified GCM to axisymmetric forcings: Applicability of the fluctuation-dissipation theorem, *J. Atmos. Sci.*, *65*, 3880–3898.

Santer, B. D., et al. (2003), Contribution of anthropogenic and natural forcing to recent tropopause height changes, *Science*, *301*, 479–483.

Schraner, M., et al. (2008), Technical note: Chemistry-climate model SOCOL: Version 2.0 with improved transport and chemistry/microphysics schemes, *Atmos. Chem. Phys.*, *8*, 5957–5974.

Scinocca, J. F., N. A. McFarlane, M. Lazare, J. Li, and D. Plummer (2008), Technical note: The CCCma third generation AGCM and its extension into the middle atmosphere, *Atmos. Chem. Phys.*, *8*, 7055–7074.

Seidel, D. J., Q. Fu, W. J. Randel, and T. J. Reichler (2008), Widening of the tropical belt in a changing climate, *Nat. Geosci.*, *1*, 21–24.

Shibata, K., and M. Deushi (2008a), Long-term variations and trends in the simulation of the middle atmosphere 1980–2004 by the chemistry-climate model of the Meteorological Research Institute, *Ann. Geophys.*, *26*, 1299–1326.

Shibata, K., and M. Deushi (2008b), Simulation of the stratospheric circulation and ozone during the recent past (1980–2004) with the MRI chemistry-climate model, *CGER Supercomputer Monogr. Rep. 13*, Natl. Inst. for Environ. Stud., Ibaraki, Japan.

Shindell, D. T., and G. A. Schmidt (2004), Southern Hemisphere climate response to ozone changes and greenhouse gas increases, *Geophys. Res. Lett.*, *31*, L18209, doi:10.1029/2004GL020724.

Simpson, I. R., M. Blackburn, and J. D. Haigh (2009), The role of eddies in driving the tropospheric response to stratospheric heating perturbations, *J. Atmos. Sci.*, *66*, 1347–1365.

Simpson, I. R., J. Haigh, M. Blackburn, and S. Sparrow (2010), The impact of the state of the troposphere on the response to stratospheric heating in a simplified GCM, *J. Clim.*, in press.

Solomon, S. (1999), Stratospheric ozone depletion: A review of concepts and history, *Rev. Geophys.*, *37*, 275–316.

Son, S.-W., and S. Lee (2005), The response of westerly jets to thermal driving in a primitive equation model, *J. Atmos. Sci.*, *62*, 3741–3757.

Son, S.-W., and S. Lee (2006), Preferred modes of variability and their relationship with climate change, *J. Clim.*, *19*, 2063–2075.

Son, S.-W., S. Lee, and S. B. Feldstein (2007), Intraseasonal variability of the zonal-mean extratropical tropopause height, *J. Atmos. Sci.*, *64*, 608–620.

Son, S.-W., L. M. Polvani, D. W. Waugh, H. Akiyoshi, R. R. Garcia, D. Kinnison, S. Pawson, E. Rozanov, T. G. Shepherd, and K. Shibata (2008), The impact of stratospheric ozone recovery on the Southern Hemisphere westerly jet, *Science*, *320*, 1486–1489.

Son, S.-W., N. F. Tandon, L. M. Polvani, and D. W. Waugh (2009a), Ozone hole and Southern Hemisphere climate change, *Geophys. Res. Lett.*, *36*, L15705, doi:10.1029/2009GL038671.

Son, S.-W., L. M. Polvani, D. W. Waugh, T. Birner, H. Akiyoshi, R. R. Garcia, A. Gettelman, D. A. Plummer, and E. Rozanov (2009b), The impact of stratospheric ozone recovery on tropopause height trends, *J. Clim.*, *22*, 429–445.

Song, Y., and W. A. Robinson (2004), Dynamical mechanism for stratospheric influences on the troposphere, *J. Atmos. Sci.*, *61*, 1711–1725.

SPARC CCMVal (2010), SPARC CCMVal report on the evaluation of chemistry-climate models, *SPARC Rep. 5*, SPARC, Toronto, Ont., Canada. (Available at http://www.atmosp.physics.utoronto.ca/SPARC)

Stenke, A., M. Dameris, V. Grewe, and H. Garny (2009), Implications of Lagrangian transport for simulations with a coupled chemistry-climate model, *Atmos. Chem. Phys.*, *9*, 5489–5504.

Teyssédre, H., et al. (2007), A new tropospheric and stratospheric chemistry and transport model MOCAGE-climat for multi-year studies: evaluation of the present-day climatology and sensitivity to surface processes, *Atmos. Chem. Phys.*, *7*, 5815–5860.

Thompson, D. W. J., and S. Solomon (2002), Interpretation of recent Southern Hemisphere climate change, *Science*, *296*, 895–899.

Thompson, D. W. J., J. M. Wallace, and G. C. Hegerl (2000), Annular modes in the extratropical circulation. Part II: Trends, *J. Clim.*, *13*, 1018–1036.

Tian, W., and M. P. Chipperfield (2005), A new coupled chemistry-climate model for the stratosphere: The importance of coupling for future O_3-climate predictions, *Q. J. R. Meteorol. Soc.*, *131*, 281–304.

Tian, W., M. P. Chipperfield, L. J. Gray, and J. M. Zawodny (2006), Quasi-biennial oscillation and tracer distributions in a coupled chemistry-climate model, *J. Geophys. Res.*, *111*, D20301, doi:10.1029/2005JD006871.

Uppala, S. M., et al. (2005), The ERA-40 reanalysis, *Q. J. R. Meteorol. Soc.*, *131*, 2961–3012.

Walker, C. C., and T. Schneider (2006), Eddy-influences on Hadley circulations: Simulation with a idealized GCM, *J. Atmos. Sci.*, *63*, 3333–3350.

Waugh, D. W., L. Oman, P. A. Newman, R. S. Stolarski, S. Pawson, J. E. Nielsen, and J. Perlwitz (2009), Effect of zonal asymmetries in stratospheric ozone on simulations of Southern Hemisphere climate, *Geophys. Res. Lett.*, *36*, L18701, doi:10.1029/2009GL040419.

Williams, G. (2006), Circulation sensitivity to tropopause height, *J. Atmos. Sci.*, *63*, 1954–1961.

Wittman, M. A. H., A. J. Charlton, and L. M. Polvani (2007), The effect of lower stratospheric shear on baroclinic instability, *J. Atmos. Sci.*, *64*, 479–496.

World Meteorological Organization (1957), Definition of the tropopause, *WMO Bull.*, *6*, 136–140.

Yin, J. H. (2005), A consistent poleward shift of the storm tracks in simulations of 21st century climate, *Geophys. Res. Lett.*, *32*, L18701, doi:10.1029/2005GL023684.

H. Akiyoshi, T. Nakamura, and Y. Yamashita, National Institute for Environmental Studies, Tsukuba, Ibaraki 305-8506, Japan.

J. Austin, Geophysical Fluid Dynamics Laboratory, NOAA, Princeton, NJ 08540, USA.

A. Baumgaertner and C. Brühl, Max Planck Institut für Chemie, D-55020 Mainz, Germany.

S. Bekki, D. Cugnet, and M. Marchand, LATMOS, Institut Pierre-Simone Laplace, UVSQ, UPMC, CNRS/INSU, F-75252 Paris, France.

P. Braesicke, O. Morgenstern, and J. Pyle, NCAS-Climate-Chemistry, Department of Chemistry, Cambridge University, Cambridge CB2 1EW, UK.

N. Butchart and S. C. Hardiman, Met Office Hadley Centre, Exeter EX1 3PB, UK.

M. P. Chipperfield, S. Dhomse, and W. Tian, School of Earth and Environment, University of Leeds, Leeds LS2 9JT, UK.

M. Dameris, V. Eyring, H. Garny, and P. Jöckel, Deutsches Zentrum für Luft- und Raumfahrt, Institut für Physik der Atmosphäre, D-82234 Wessling, Oberpfaffenhofen, Germany.

S. Frith, NASA Goddard Space Flight Center, Greenbelt, MD 20771, USA.

R. Garcia and J. F. Lamarque, Atmospheric Chemistry Division, National Center for Atmospheric Research, Boulder, CO 80307, USA.

E. P. Gerber, Center for Atmosphere Ocean Science, Courant Institute of Mathematical Sciences, New York University, New York, NY 10012, USA.

N. P. Gillett and J. F. Scinocca, Canadian Centre for Climate Modelling and Analysis, Environment Canada, University of Victoria, Victoria, BC V8W 2Y2, Canada.

E. Mancini and G. Pitari, Dipartimento di Fisica, Universita degli Studi de L'Aquila, I-67010 Coppito, L'Aquila, Italy.

M. Michou and H. Teyssèdre, GAME/CNRM, Météo-France, Centre National de Recherches Météorologiques, F-31057 Toulouse, France.

J. Perlwitz, Physical Sciences Division, Earth System Research Laboratory, NOAA, Boulder, CO 80305, USA.

D. A. Plummer, Canadian Centre for Climate Modelling and Analysis, Environment Canada, Toronto, ON V8W 3V6, Canada.

L. M. Polvani, Department of Applied Physics and Applied Mathematics, Columbia University, New York, NY 10027, USA.

E. Rozanov, Physikalisch-Meteorologisches Observatorium Davos/World Radiation Center, CH-7260 Davos, Switzerland.

K.-H. Seo, Department of Atmospheric Sciences, Pusan National University, Pusan 609-735, South Korea.

T. G. Shepherd, Department of Physics, University of Toronto, Toronto, ON M5S 1A7, Canada.

K. Shibata, Meteorological Research Institute, Tsukuba, Ibaraki 305-0052, Japan.

D. Smale, National Institute of Water and Atmospheric Research, Lauder, Central Otago 9320, New Zealand.

S.-W. Son, Department of Atmospheric and Oceanic Sciences, McGill University, 805 Sherbrooke St. West, Montreal, QC H3A 2K6, Canada. (seok-woo.son@mcgill.ca)

D. Waugh, Department of Earth and Planetary Sciences, Johns Hopkins University, Baltimore, MD 21218, USA.